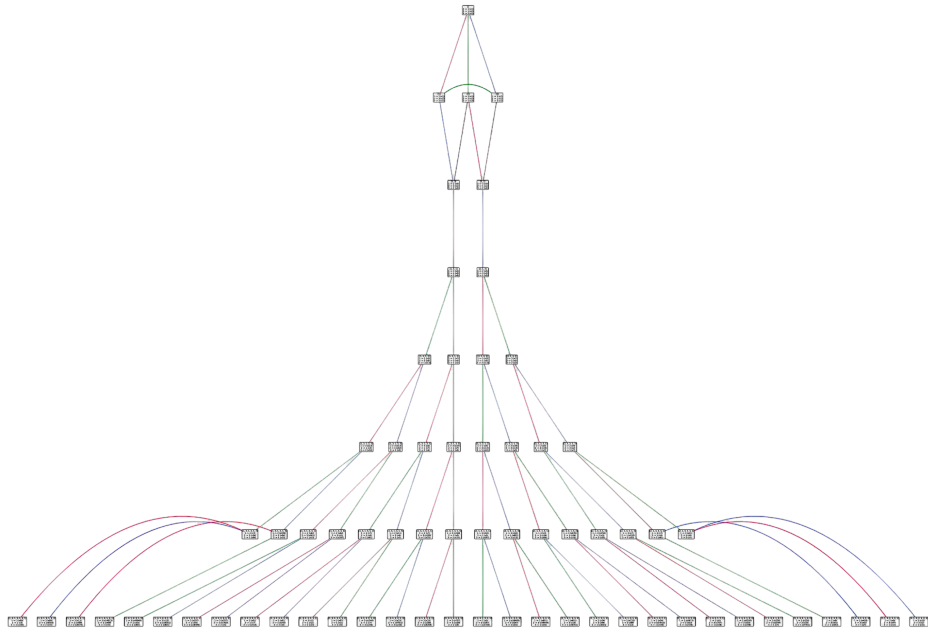


Math 635: Cluster Varieties

Algebra, Topology, Geometry, Duality

Kyler Siegel
USC Spring 2026
https://kylersiegel.xyz/635_spring_2026.html



Disclaimer: These notes are based on handwritten lecture notes which were typeset and lightly edited with AI assistance. This typesetting process is not perfect and could have introduced some errors.

Contents

| | |
|--|----------|
| 1 Lecture 1 | 4 |
| 1.1 Introduction | 4 |
| 1.2 Total Positivity | 5 |
| 1.3 Plücker Coordinates on Grassmannians | 6 |
| 1.4 Positivity Testing for $\text{Gr}_{2,m}$ | 6 |
| 2 Lecture 2 | 9 |
| 2.1 Flag Positivity | 9 |
| 2.2 Wiring Diagrams | 10 |

| | |
|---|-----------|
| 3 Lecture 3 | 11 |
| 3.1 The Flag Variety and Basic Affine Space | 11 |
| 3.2 Checking Total Positivity for $n \times n$ Matrices | 12 |
| 3.3 Quivers and Their Mutation | 12 |
| 3.4 Triangulations and Quivers | 13 |
| 4 Lecture 4 | 14 |
| 4.1 Review: Triangulations and Quivers | 14 |
| 4.2 Wiring Diagrams and Quivers | 14 |
| 4.3 Plabic Graphs | 16 |
| 4.4 Quivers from Plabic Graphs | 16 |
| 4.5 Moves on Plabic Graphs | 17 |
| 4.6 Mutation Equivalence | 17 |
| 4.7 Finite Mutation Type | 18 |
| 5 Lecture 5 | 19 |
| 5.1 Extended Exchange Matrices | 19 |
| 5.2 Matrix Mutation | 21 |
| 5.3 Skew-Symmetrizable Matrices | 21 |
| 5.4 Diagrams and Uniqueness | 22 |
| 5.5 Mutation Equivalence for Matrices | 23 |
| 5.6 Labeled Seeds | 24 |
| 6 Lecture 6 | 25 |
| 6.1 Labeled Seeds and Seed Mutation | 25 |
| 6.2 Examples | 25 |
| 6.3 Seed Patterns and Cluster Algebras | 26 |
| 6.4 Examples of Cluster Algebras | 26 |
| 7 Lecture 7 | 27 |
| 7.1 Rank 1 Cluster Algebras | 27 |
| 7.2 Rank 2 Cluster Algebras | 29 |
| 8 Lecture 8 | 32 |
| 8.1 Rank 2 examples (continued) | 32 |
| 8.2 The Laurent phenomenon | 33 |
| 8.3 Markov triples | 34 |
| 8.4 The Markov tree | 35 |
| 8.5 The Somos-4 sequence | 35 |
| 9 Lecture 9 | 37 |
| 9.1 The \hat{y} -variables | 37 |
| 9.2 Y-seeds | 38 |
| 9.3 Semifields | 38 |
| 9.4 Coefficient tuples and tropical Y-seed mutation | 39 |

| | |
|--|-----------|
| 10 Lecture 10 | 41 |
| 10.1 Alternative characterization of labeled seeds | 41 |
| 10.2 Example: A_2 revisited | 41 |
| 10.3 Finite type classification in rank 2 | 42 |
| 10.4 2-finiteness | 44 |
| 11 Lecture 11 | 45 |
| 11.1 Cartan matrices and Dynkin diagrams | 45 |
| 11.2 Finite type classification | 46 |
| 12 Lecture 12 | 48 |
| 12.1 Bordered surfaces with marked points | 48 |
| 12.2 Teichmüller space and lambda lengths | 49 |
| 12.3 Exchange matrices from triangulations | 52 |
| 12.4 Examples | 53 |
| 13 Lecture 13 | 57 |
| 13.1 More examples of cluster algebras from surfaces | 57 |
| 13.2 Rank 3 surface-type cluster algebras | 59 |
| 13.3 Non-surface-type quivers and infinite mutation type | 60 |
| 14 Lecture 14 | 62 |
| 14.1 Forks and the tree lemma | 62 |
| 14.2 Exchange graphs of forks | 64 |
| 14.3 Mutation-infinite quivers and forks | 65 |
| 14.4 Exchange graphs of mutation-cyclic 3-vertex quivers | 65 |
| 14.5 Alternating mutations | 67 |

1 Lecture 1

Date: January 12, 2026

Main reference: [FWZ21], §1–2.

1.1 Introduction

Roughly speaking:

- A **cluster variety** is a complex algebraic variety obtained by gluing together many copies of $(\mathbb{C}^*)^n$, where the gluing maps take a very particular form.
- A **cluster algebra** is the algebra of regular functions $f: V \rightarrow \mathbb{C}$ on a cluster variety.

Fomin–Zelevinsky, early 2000s: Introduced cluster algebras. They arise in many parts of mathematics and physics as a kind of “universal model” for mutation/wall-crossing phenomena:

- Quiver representation theory
- Teichmüller theory
- Poisson geometry
- Grassmannians
- Total positivity
- QFT scattering amplitudes (amplituhedron)
- Integrable systems
- String theory (BPS states)
- etc.

Gross–Hacking–Keel–Kontsevich (GHKK) [Gro+18]:

- Constructed canonical bases for cluster algebras.
- Established positivity of the Laurent phenomenon.
- Proof uses mirror symmetry for log Calabi–Yau varieties (which can be thought of as a generalization of toric varieties, related to almost toric fibrations in symplectic geometry).
- Many strong applications in representation theory, e.g., canonical bases for finite-dimensional irreducible representations of $\mathrm{SL}_n(\mathbb{C})$.

Remark 1.1. The canonical bases were originally found independently by Lusztig and Kashiwara in the early 1990s using quantum groups. Amazingly, the construction of GHKK uses only general geometry—no representation theory!

1.2 Total Positivity

Definition 1.2. A matrix $A \in \text{Mat}_{n \times n}(\mathbb{R})$ is **totally positive** (TP) if all of its minors are positive.

Gantmacher–Krein (1930s): If A is TP, then the eigenvalues of A are real, positive, and distinct.

Binet–Cauchy theorem: The TP matrices are closed under multiplication, and hence form a multiplicative semigroup $G_{>0}$.

Lusztig: Extended the definition of $G_{>0}$ to other semisimple Lie groups G .

More generally: If a given complex algebraic variety Z has a distinguished family Δ of regular functions $Z \rightarrow \mathbb{C}$, we define the **TP variety** by

$$Z_{>0} := \{z \in Z \mid f(z) > 0 \text{ for all } f \in \Delta\}.$$

Example 1.3. For $Z = \text{Mat}_{n \times n}(\mathbb{C})$, $\text{GL}_n(\mathbb{C})$, or $\text{SL}_n(\mathbb{C})$, we recover the above notion of TP, where $\Delta = \{\text{minors}\}$.

Example 1.4. The **Grassmannian** $\text{Gr}_{k,m}(\mathbb{C}) = \{k\text{-dimensional linear subspaces of } \mathbb{C}^m\}$, with $\Delta = \{\text{Plücker coordinates}\}$.

Example 1.5. Partial flag manifolds, homogeneous spaces for semisimple complex Lie groups, etc. (slight scaling ambiguity).

Lemma 1.6. A matrix $A \in \text{Mat}_{n \times n}$ has $\binom{2n}{n} - 1$ minors.

Proof. The number of minors is

$$\# = \sum_{k=1}^n \binom{n}{k}^2.$$

By Vandermonde's identity:

$$\binom{m+w}{r} = \sum_{k=0}^r \binom{m}{k} \binom{w}{r-k}.$$

Setting $m = w = r = n$ gives

$$\binom{2n}{n} = \sum_{k=0}^n \binom{n}{k}^2,$$

from which the result follows. \square

Remark 1.7. To verify Vandermonde's identity, note that both sides count the number of subcommittees with r members, given a committee with m men and w women.

Question 1.8. Can we check that $A \in \text{Mat}_{n \times n}$ is TP by only testing a subset of the $\binom{2n}{n} - 1$ minors? How many tests are needed?

Example 1.9. Let $A = \begin{pmatrix} a & b \\ c & d \end{pmatrix} \in \text{Mat}_{2 \times 2}$. Define $\delta := ad - bc$, so $d = \frac{\delta+bc}{a}$. Thus, if $a, b, c, \delta > 0$, then d is automatically positive. This reduces $\binom{4}{2} - 1 = 5$ checks to 4 checks.

The goal is “efficient TP testing.”

1.3 Plücker Coordinates on Grassmannians

Given $A \in \text{Mat}_{k \times m}$ of rank k , we have $\text{rowspan}(A) =: [A] \in \text{Gr}_{k,m}$.

For $J \subseteq \{1, \dots, m\}$ with $|J| = k$, the **Plücker coordinate** is

$$P_J(A) := k \times k \text{ minor of } A \text{ corresponding to columns } J.$$

Note 1.10. For $A, B \in \text{Mat}_{k \times m}$ with $[A] = [B]$ (i.e., same row spans), the tuples $(P_J(A))_{|J|=k}$ and $(P_J(B))_{|J|=k}$ agree up to common rescaling. We thus get a map

$$\text{Gr}_{k,m} \longrightarrow \mathbb{CP}^{N-1}, \quad N = \binom{m}{k}.$$

In fact, this is an embedding, called the **Plücker embedding**.

Let $\mathbb{C}[\text{Mat}_{k \times m}]$ denote the coordinate ring of $\text{Mat}_{k \times m}$, i.e., the polynomial algebra in variables x_{ij} for $1 \leq i \leq k$, $1 \leq j \leq m$.

Definition 1.11. The **Plücker ring** $R_{k,m}$ is the subring of $\mathbb{C}[\text{Mat}_{k \times m}]$ generated by P_J over all $J \in \{1, \dots, m\}$ with $|J| = k$.

Claim 1.12. *The ideal of relations in $R_{k,m}$ is generated by certain quadratic relations called the Grassmann–Plücker relations.*

Definition 1.13. The **totally positive Grassmannian** $\text{Gr}_{k,m}^+$ is the subset of $\text{Gr}_{k,m}$ consisting of those points whose Plücker coordinates are all positive (up to common scaling).

Note 1.14. For $A \in \text{Mat}_{k \times m}(\mathbb{R})$, we have $[A] \in \text{Gr}_{k,m}^+$ if and only if all $k \times k$ minors of A have the same sign.

Question 1.15. For $A \in \text{Mat}_{k \times m}(\mathbb{R})$, can we verify that all $k \times k$ minors are positive by only checking a subset of the $\binom{m}{k}$ minors? How many tests are needed?

(We may assume positive WLOG by rescaling.)

1.4 Positivity Testing for $\text{Gr}_{2,m}$

Claim 1.16. *Given $A \in \text{Mat}_{2 \times m}$, put $P_{ij} := P_{\{i,j\}}$ for $1 \leq i < j \leq m$. To check that all 2×2 minors $P_{ij}(A) > 0$, it suffices to check only the $2m - 3$ special ones.*

Note 1.17. $2m - 3 = \dim \text{Gr}_{2,m} + 1$.

Lemma 1.18. *For $1 \leq i < j < k < \ell \leq m$, we have the three-term Grassmann–Plücker relation:*

$$P_{ik}P_{j\ell} = P_{ij}P_{k\ell} + P_{i\ell}P_{jk}.$$

Remark 1.19. For an inscribed quadrilateral (Figure 1), Ptolemy’s theorem (2nd century) gives

$$AC \cdot BD = AB \cdot CD + BC \cdot AD.$$

Example 1.20. Let $A = \begin{pmatrix} a & b & c & d \\ e & f & g & h \end{pmatrix}$. We verify $P_{13}P_{24} = P_{12}P_{34} + P_{14}P_{23}$, i.e.,

$$(ag - ce)(bh - df) = (af - be)(ch - dg) + (ah - de)(bg - cf). \quad \checkmark$$

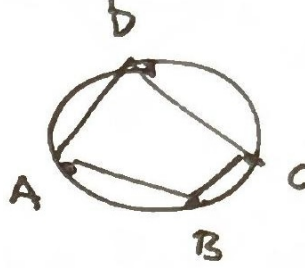


Figure 1: Inscribed quadrilateral for Ptolemy's theorem.

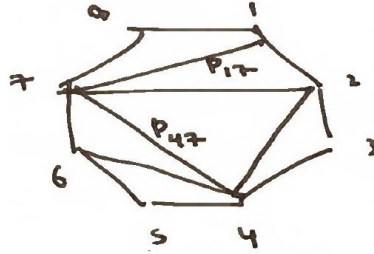


Figure 2: A triangulated polygon \mathbb{P}_m with vertices labeled $1, \dots, m$.

Put \mathbb{P}_m = regular m -gon, and let T be a triangulation.

To each side or diagonal, associate P_{ij} , where i, j are the endpoints.

- **Cluster variables:** P_{ij} ranging over diagonals.
- **Frozen variables:** P_{ij} ranging over sides.
- **Extended cluster:** $\{\text{cluster vars}\} \cup \{\text{frozen vars}\} =: \tilde{x}(T)$.

Note 1.21. The extended cluster has $2m - 3$ variables, and we claim that these are algebraically independent.

Example 1.22. In Figure 2, we have cluster variables $P_{17}, P_{27}, P_{47}, P_{24}$ and frozen variables $P_{12}, P_{23}, \dots, P_{78}, P_{18}$.

Theorem 1.23. *Each P_{ij} for $1 \leq i < j \leq n$ can be written as a subtraction-free rational expression in the elements of a given extended cluster $\tilde{x}(T)$.*

Corollary 1.24. *If each $P_{ij} \in \tilde{x}(T)$ evaluates positively on a given $A \in \text{Mat}_{2 \times m}$, then all of the $2m - 3$ of the $\binom{m}{2}$ minors of A are positive.*

Proof of Theorem. Follows by combining:

- (1) Each P_{ij} appears as an element of an extended cluster $\tilde{x}(T)$ for some triangulation T of \mathbb{P}_m .
- (2) Any two triangulations of \mathbb{P}_m are related by a sequence of **flips** (see Figure 3).
- (3) For a flip, replace P_{ik} with $P_{j\ell}$. Using the three-term GP relation, we have

$$P_{ik} = \frac{P_{ij}P_{k\ell} + P_{i\ell}P_{jk}}{P_{j\ell}}.$$

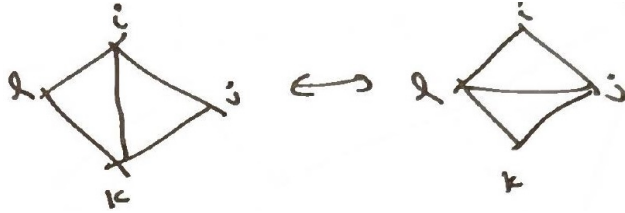


Figure 3: A flip replaces one diagonal with another in a quadrilateral.

Remark 1.25. In fact, each Plücker coordinate P_{ij} can be written as a Laurent polynomial with positive coefficients in the Plücker coordinates from $\tilde{x}(T)$. This is an example of the **positive Laurent phenomenon**.

The combinatorics of flips is encoded by a graph:

- Vertices are triangulations.
- Edges are flips.

Each vertex has degree $m - 3$. In fact, this is the 1-skeleton of an $(m - 3)$ -dimensional convex polytope called the **associahedron** (discovered by Stasheff); see Figures 4 and 5.

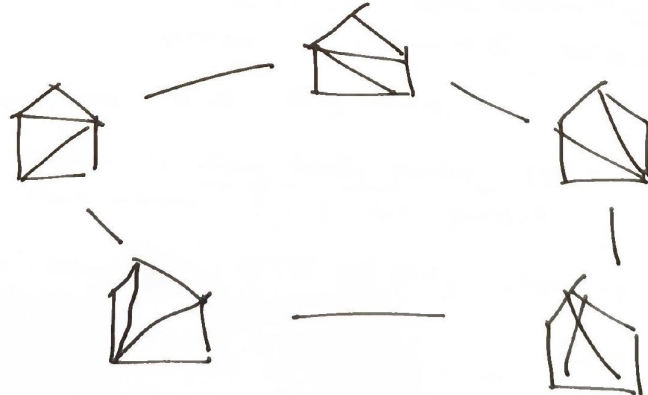


Figure 4: The associahedron for $m = 5$ (a pentagon).

Definition 1.26. A **cluster monomial** is a monomial in the variables of a given extended cluster $\tilde{x}(T)$.

Theorem 1.27 (19th century invariant theory). *The set of all cluster monomials gives a linear basis for the Plücker ring $R_{2,m}$.*

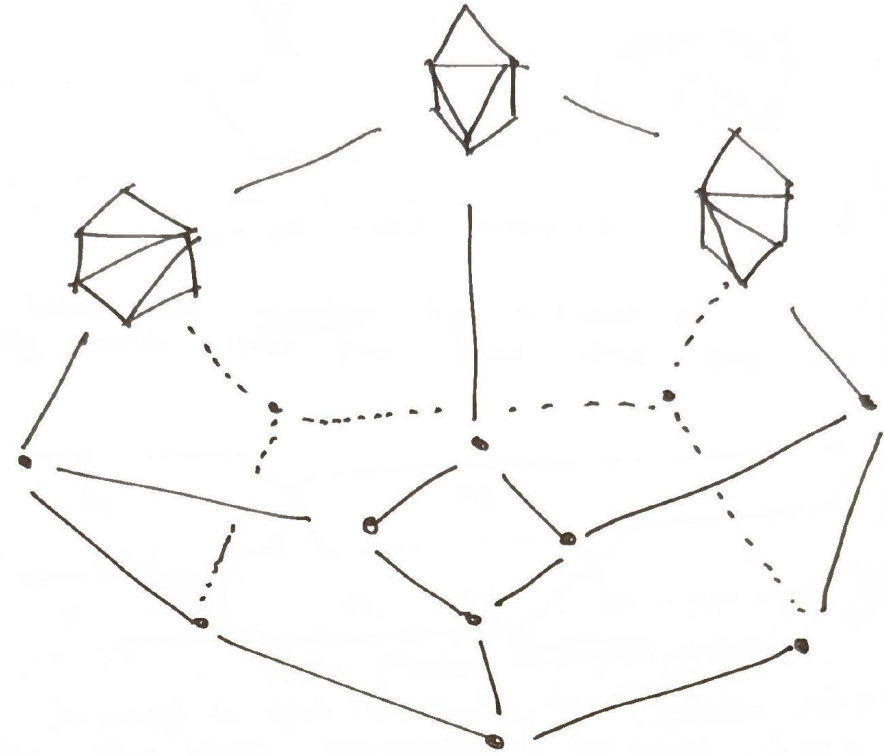


Figure 5: The associahedron for $m = 6$ (a 3-dimensional polytope).

2 Lecture 2

Date: January 14, 2026

Main reference: [FWZ21], §2–3.

2.1 Flag Positivity

Before moving to TP for $n \times n$ matrices, we discuss an intermediate notion called “flag positivity.” Put $G = \mathrm{SL}_n$.

Definition 2.1. Given $J \subsetneq \{1, \dots, n\}$ nonempty, the **flag minor** P_J is the function $P_J: G \rightarrow \mathbb{C}$ defined by

$$P_J(z) := z(\vec{e}_J) \mapsto \det(z_{\alpha\beta} \mid \alpha \leq |J|, \beta \in J),$$

i.e., the $|J| \times |J|$ minor which is “top-justified.”

Note 2.2. There are $2^n - 2$ flag minors.

Definition 2.3. An element $z \in G$ is **flag totally positive** (FTP) if all flag minors $P_J(z)$ are positive.

Question 2.4. Can we check FTP by only checking a subset of the $2^n - 2$ flag minors?

Claim 2.5. It suffices to check only $\frac{(n-1)(n+2)}{2}$ special flag minors.

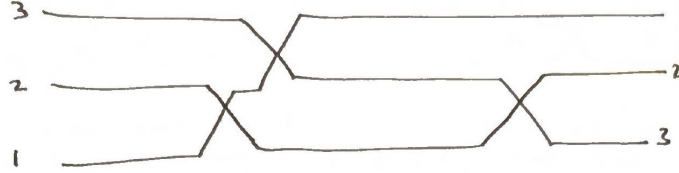


Figure 6: A wiring diagram for $n = 3$: each pair of lines intersect exactly once.

2.2 Wiring Diagrams

Each pair of lines intersect exactly once (Figure 6).

We label each **chamber** by a subset of $\{1, \dots, n\}$ indicating which lines pass below that chamber (see Figure 7).

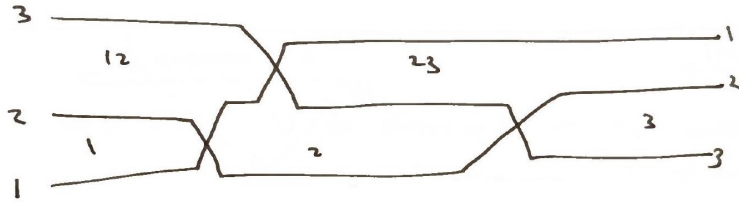


Figure 7: A wiring diagram with chamber labels.

Note 2.6. There are always $\frac{(n-1)(n+2)}{2}$ chambers.

Associated to each chamber is its **chamber minor** P_J , the flag minor corresponding to its subset $J \subsetneq \{1, \dots, n\}$.

Extended cluster: All chamber minors of a wiring diagram.

- **Cluster variables:** the chamber minors for bounded chambers. There are $\frac{(n-1)n}{2}$ of these.
- **Frozen variables:** the chamber minors for unbounded chambers. There are $2n - 2$ of these.

Theorem 2.7. Every flag minor can be written as a subtraction-free rational expression in the chamber minors of a given wiring diagram.

Corollary 2.8. If the $\frac{(n-1)(n+2)}{2}$ chamber minors evaluate positively at a matrix $z \in \mathrm{SL}_n$, then z is **FTP**.

Proof outline. Follows by:

- (1) Each flag minor appears as a chamber minor in some wiring diagram.
- (2) Any two wiring diagrams can be transformed into each other by a sequence of local **braid moves** (see Figure 8).
- (3) Under each braid move, the collection of chamber minors changes by exchanging $Y \leftrightarrow Z$, and we have

$$YZ = AC + BD.$$

□

Remark 2.9. In fact, each flag minor can be written as a Laurent polynomial with positive coefficients in the chamber minors of a given wiring diagram.

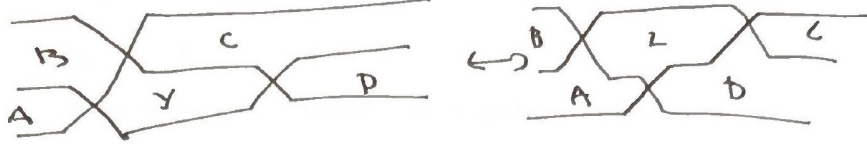


Figure 8: A braid move exchanges two adjacent crossings.

3 Lecture 3

Date: January 23, 2026

Main reference: [FWZ21], §1.3, §1.4, §2.1.

3.1 The Flag Variety and Basic Affine Space

Put $G = \mathrm{SL}_n(\mathbb{C})$. Let $B \subset G$ denote the subgroup of lower triangular matrices (the Borel subgroup), and let $U \subset G$ denote the subgroup of unipotent lower triangular matrices, i.e., lower triangular matrices with 1's on the diagonal:

$$U = \left\{ \begin{pmatrix} 1 & 0 & \cdots & 0 \\ * & 1 & \cdots & 0 \\ \vdots & \vdots & \ddots & \vdots \\ * & * & \cdots & 1 \end{pmatrix} \right\}.$$

Note 3.1. As a variety, $U \cong \mathbb{C}^{n(n-1)/2}$.

Similarly, let U^+ denote the subgroup of unipotent upper triangular matrices.

Definition 3.2. The (complete) **flag variety** is

$$\mathcal{F}\ell = B \backslash G = \{V_1 \subset V_2 \subset \cdots \subset V_{n-1} \subset \mathbb{C}^n \mid \dim V_i = i\}.$$

This is identified with the homogeneous space $B \backslash G$, where B acts on G by left multiplication.

Definition 3.3. The **basic affine space** is $U \backslash G$, where U acts on G by left multiplication.

Note 3.4. There is a natural projection $U \backslash G \rightarrow B \backslash G$, which is a $(\mathbb{C}^*)^{n-1}$ -bundle (a torus bundle) over the flag variety.

Let $\mathbb{C}[G]$ denote the coordinate ring of $G = \mathrm{SL}_n(\mathbb{C})$, and let $\mathbb{C}[G]^U$ denote the ring of U -invariant polynomials, where U acts by left multiplication on matrix entries.

Claim 3.5 (First and Second Fundamental Theorems of Invariant Theory).

- (1) $\mathbb{C}[G]^U$ is generated by flag minors.
- (2) The ideal of relations among flag minors in $\mathbb{C}[G]^U$ is generated by the **generalized Plücker relations**.

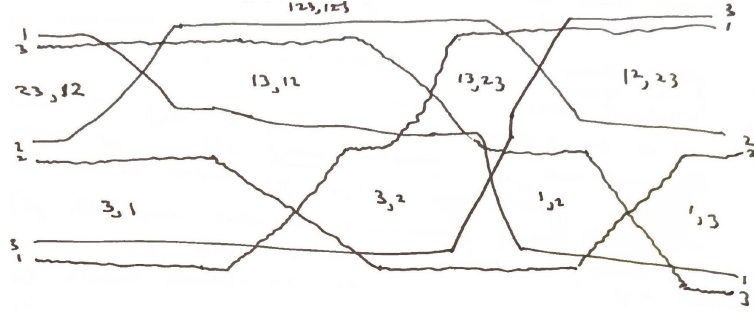


Figure 9: A double wiring diagram for $n = 3$.

3.2 Checking Total Positivity for $n \times n$ Matrices

Given $I, J \subseteq \{1, \dots, n\}$ of some cardinality, let Δ_J^I denote the minor of an $n \times n$ matrix determined by rows in I and columns in J . This extends to flag minors when $|I| = |J|$.

Double wiring diagrams: These are a generalization of the wiring diagrams from Lecture 2, used to study total positivity for $n \times n$ matrices (see Figure 9).

Claim 3.6. *Every minor Δ_J^I of a chamber can be written as a subtraction-free rational expression in the chamber minors of a given double wiring diagram.*

Claim 3.7. *Every minor is a chamber minor for some double wiring diagram.*

The proof follows from:

- (1) Any two double wiring diagrams can be linked by local moves.
- (2) Each local move relates chamber minors of different diagrams.
- (3) Each local double move satisfies a relation of the form $YZ = AC + BD$.

Remark 3.8. The graph with vertices given by double wiring diagrams and edges given by local moves is related to the theory of cluster algebras.

Remark 3.9. In fact, each minor can be written as a Laurent polynomial with positive coefficients in the chamber minors.

3.3 Quivers and Their Mutation

Definition 3.10. A **quiver** Q is a finite directed graph (see Figure 10) with:

- No loops (no arrows $i \rightarrow i$).
- No 2-cycles (no pairs of arrows $i \Rightarrow j$ going both directions).



Figure 10: Examples of quivers (valid examples marked \checkmark , invalid example marked \times).

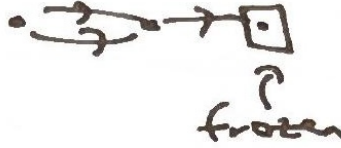


Figure 11: An ice quiver with frozen vertices indicated by boxes.

Definition 3.11. An **ice quiver** is a quiver in which some vertices are designated as “frozen” (see Figure 11), and there are no arrows between two frozen vertices. The non-frozen vertices are called **mutable**.

Definition 3.12. Let Q be an ice quiver and let k be a mutable vertex. The **mutation** $\mu_k(Q) = Q'$ at vertex k is defined as follows (see Figure 12):

- (1) For each path $i \rightarrow k \rightarrow j$, add an arrow $i \rightarrow j$ (unless i, j are both frozen).
- (2) Reverse the direction of all arrows incident to k .
- (3) Remove any 2-cycles that were created.

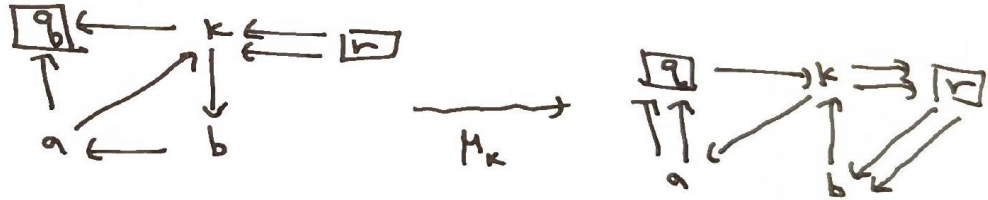


Figure 12: Illustration of quiver mutation at a vertex.

Exercise 3.13.

- (1) Mutation is an involution, i.e., $\mu_k(\mu_k(Q)) = Q$.
- (2) Mutation commutes with reversing the orientations of all arrows.
- (3) If k, ℓ are mutable vertices with no arrows between them, then mutations commute:

$$\mu_k(\mu_\ell(Q)) = \mu_\ell(\mu_k(Q)).$$

Remark 3.14. If k is a sink or source, then μ_k simply reverses all arrows incident to k .

Exercise 3.15. For any quiver Q that is a tree with no frozen vertices, show that one can get from any orientation to any other orientation by a sequence of mutations at sources and sinks.

3.4 Triangulations and Quivers

We can assign to each triangulation T of the polygon \mathbb{P}_m a quiver $Q(T)$ (see Figure 13).

Exercise 3.16. If T' is obtained from T by a flip along diagonal γ , then

$$Q(T') = \mu_\gamma(Q(T)).$$

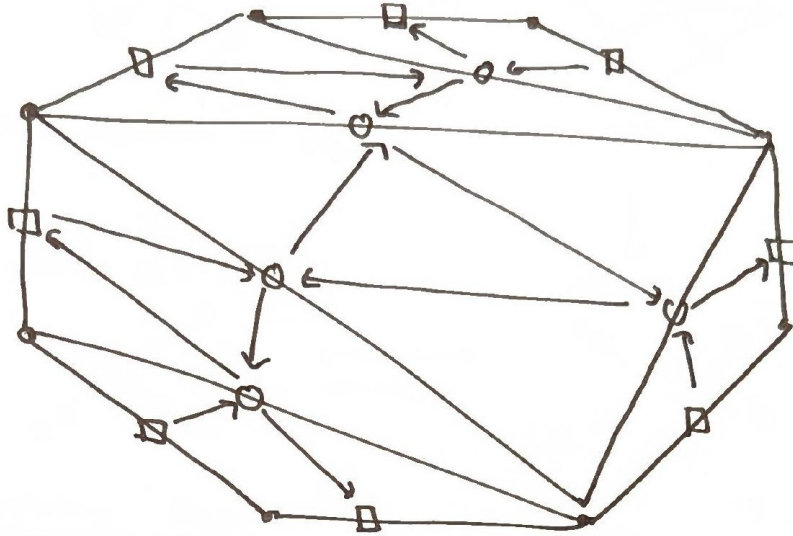


Figure 13: A triangulation T of \mathbb{P}_m and its associated quiver $Q(T)$.

4 Lecture 4

Date: January 26, 2026

Main reference: [FWZ21], §2.2, §2.3, §2.4, §2.5, §2.6.

4.1 Review: Triangulations and Quivers

Example 4.1. Let T be a triangulation of \mathbb{P}_4 . Then a flip along a diagonal gives a new triangulation T' (see Figure 14):



Figure 14: A flip between triangulations T and T' of \mathbb{P}_4 , and the corresponding quivers $Q(T)$ and $Q(T')$ related by mutation.

4.2 Wiring Diagrams and Quivers

Given a wiring diagram D , we can associate a quiver $Q(D)$ (see Figure 15).

Vertices: The vertices of $Q(D)$ are the chambers of D . A vertex is mutable if the corresponding chamber is bounded, and frozen otherwise.

Arrows: For chambers c, c' , we have an arrow $c \rightarrow c'$ in $Q(D)$ if one of the following holds (see Figure 16):

- (i) The right end of c equals the left end of c' .

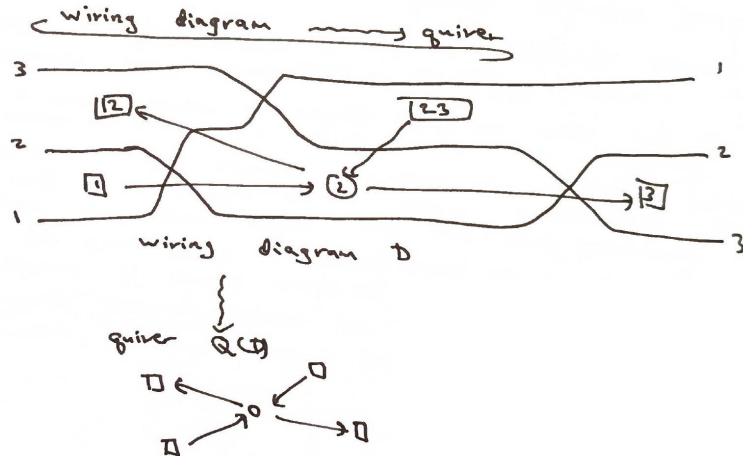


Figure 15: A wiring diagram D and its associated quiver $Q(D)$.

- (ii) The left end of c is directly above c' , and the right end of c' is directly below c .
- (iii) The left end of c is directly below c' , and the right end of c' is directly above c .

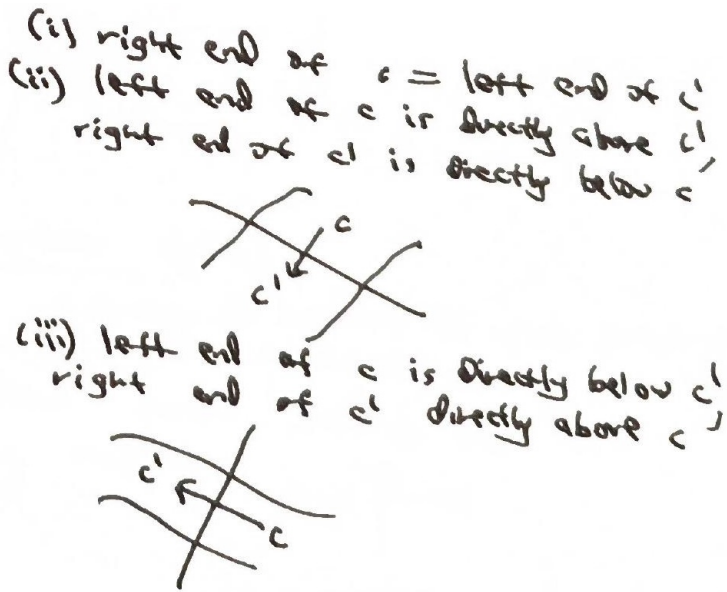


Figure 16: The arrow rules for chambers in a wiring diagram.

Exercise 4.2. If D, D' are wiring diagrams related by a braid move at chamber Y , then

$$Q(D') = \mu_Y(Q(D)).$$

Example 4.3. Figure 17 shows two wiring diagrams related by a braid move, and the corresponding quivers related by mutation at the central chamber.

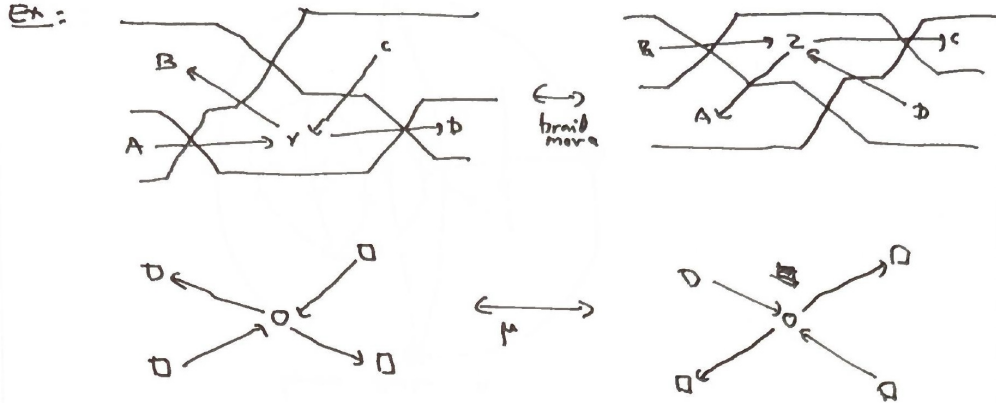


Figure 17: A braid move on wiring diagrams and the corresponding quiver mutation.

4.3 Plabic Graphs

Remark 4.4. We also have an assignment

$$\text{double wiring diagram } D \rightsquigarrow \text{quiver } Q(D).$$

The description is more complicated, but it is a special case of the quiver associated to a planar bipartite graph.

Definition 4.5. A **plabic graph** G is a connected planar bipartite graph embedded in a disk, where:

- Each vertex is colored black or white and lies either in the interior of the disk or on its boundary.
- Each edge connects vertices of different colors and is a simple curve whose interior is disjoint from the other edges and the disk boundary.
- For each face (connected component of complement), the closure is simply connected.
- Each interior vertex has degree ≥ 2 .
- Each boundary vertex has degree 1.

Note 4.6. We consider plabic graphs up to isotopy; see Figure 18 for an example.

4.4 Quivers from Plabic Graphs

Given a plabic graph G , we can associate a quiver $Q(G)$:

Vertices: The vertices of $Q(G)$ are the faces of G . A vertex is frozen if the corresponding face is incident to the disk boundary, and mutable otherwise.

Arrows: For each edge of G , we have an arrow joining the two faces it separates, using the orientation rule shown in Figure 19:

Finally, remove oriented 2-cycles.

Example 4.7. Figure 20 shows a plabic graph G and the construction of its quiver $Q(G)$.

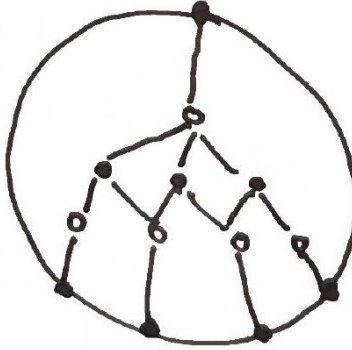


Figure 18: An example of a plabic graph.



Figure 19: The orientation rule for arrows: the arrow points so that the white vertex is on the left.

4.5 Moves on Plabic Graphs

Definition 4.8. Say a vertex v is **bivalent** if it is adjacent to two interior vertices.

Remark 4.9. Contracting or decontracting a bivalent vertex (Figure 21) does not change the associated quiver.

Definition 4.10. Say G has a **quadrilateral** if it has a face whose vertices have degree ≥ 3 .

Exercise 4.11. If G, G' are related by a spider move (Figure 22), then $Q(G), Q(G')$ are related by mutation.

Example 4.12. Figure 23 shows two plabic graphs related by a spider move, and the corresponding quivers.

4.6 Mutation Equivalence

Definition 4.13. Two quivers Q, Q' are **mutation equivalent** if Q becomes isomorphic to Q' after a sequence of mutations.

Definition 4.14. Put

$$[Q] := \{\text{all quivers which are mutation equivalent to } Q\}/\text{isomorphism}.$$

Example 4.15. Let Q be the A_3 quiver (three vertices in a line):

$$\bullet \rightarrow \bullet \rightarrow \bullet$$

Then $[Q]$ has 4 elements (Figure 24):

Exercise 4.16. Show that $[Q]$ has exactly 4 elements for Q the A_3 quiver.

Example 4.17. Let Q be the “Markov quiver” (Figure 25):

In fact, $[Q]$ is just a single element (the Markov quiver is mutation equivalent only to itself).

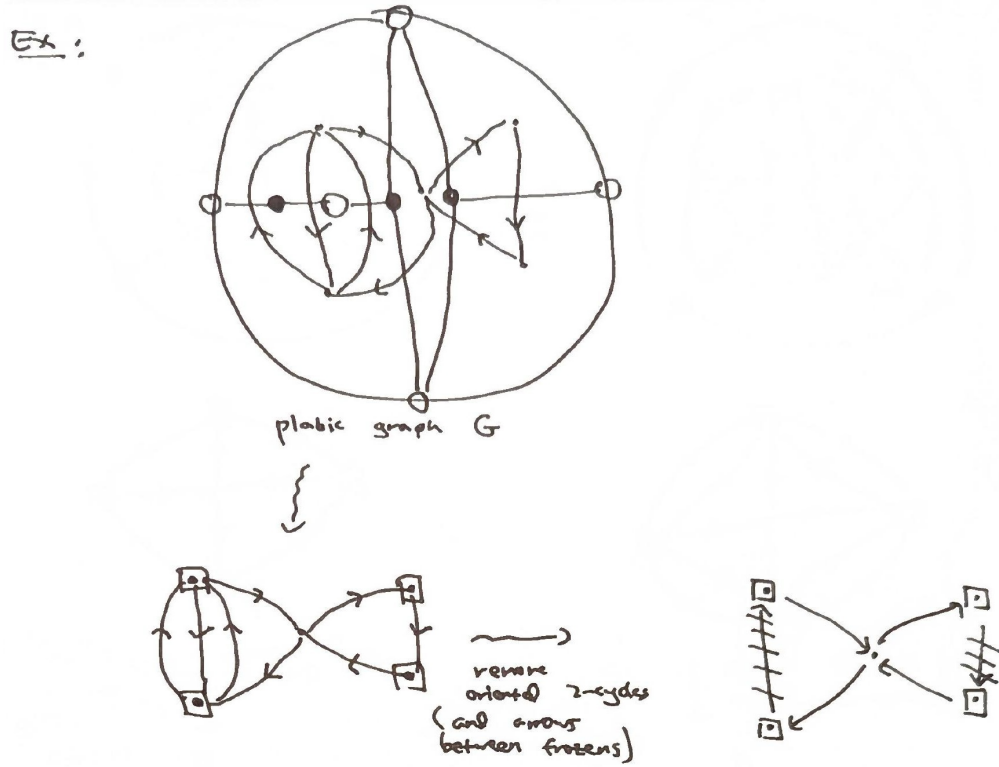


Figure 20: A plabic graph G and its associated quiver $Q(G)$, after removing oriented 2-cycles and arrows between frozen vertices.

4.7 Finite Mutation Type

Definition 4.18. A quiver Q has **finite mutation type** if $[Q]$ is finite.

Remark 4.19. There is a classification theorem for quivers with no frozen vertices and finite mutation type.

Definition 4.20. A quiver Q is **acyclic** if it has no oriented cycles.

Theorem 4.21 (Caldero–Keller '06). *If Q, Q' are acyclic and mutation equivalent, then we can transform Q into Q' by a sequence of mutations at sources and sinks. In particular, Q and Q' have the same underlying undirected graphs.*

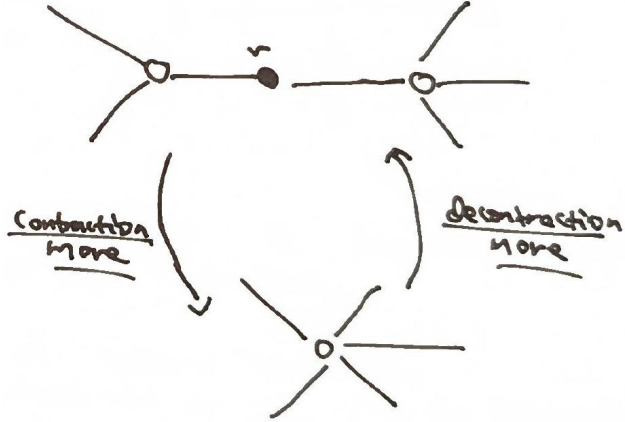


Figure 21: Contraction and decontraction moves on a bivalent vertex.

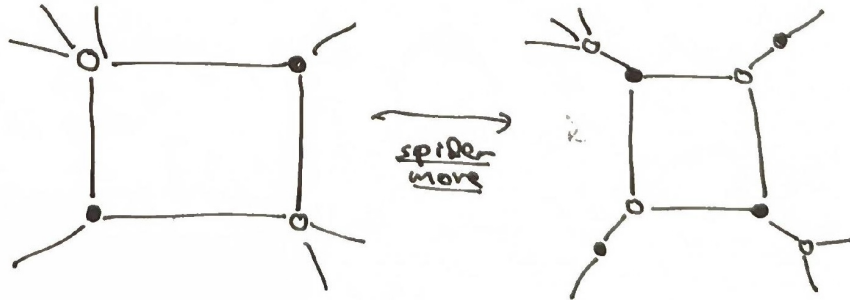


Figure 22: The spider move on a quadrilateral face.

5 Lecture 5

Date: January 28, 2026

Main reference: [FWZ21], §2.7, §2.8.

5.1 Extended Exchange Matrices

Definition 5.1. Let Q be a quiver with vertices labeled by $1, \dots, m$, such that $1, \dots, n$ are the **mutable** vertices (with $n \leq m$). The **extended exchange matrix** is

$$\tilde{B}(Q) = (b_{ij})_{\substack{1 \leq i \leq m \\ 1 \leq j \leq n}}, \quad \text{where} \quad b_{ij} = \begin{cases} \ell & \text{if } \ell \text{ arrows } i \rightarrow j \\ -\ell & \text{if } \ell \text{ arrows } j \rightarrow i \\ 0 & \text{else} \end{cases}$$

This is an $m \times n$ matrix. The **exchange matrix** is the submatrix

$$B(Q) := (b_{ij})_{1 \leq i, j \leq n},$$

which is an $n \times n$ skew-symmetric matrix.

Example 5.2. Consider the quiver Q with mutable vertices 1, 2, 3 and frozen vertices 4, 5 (Figure 26):

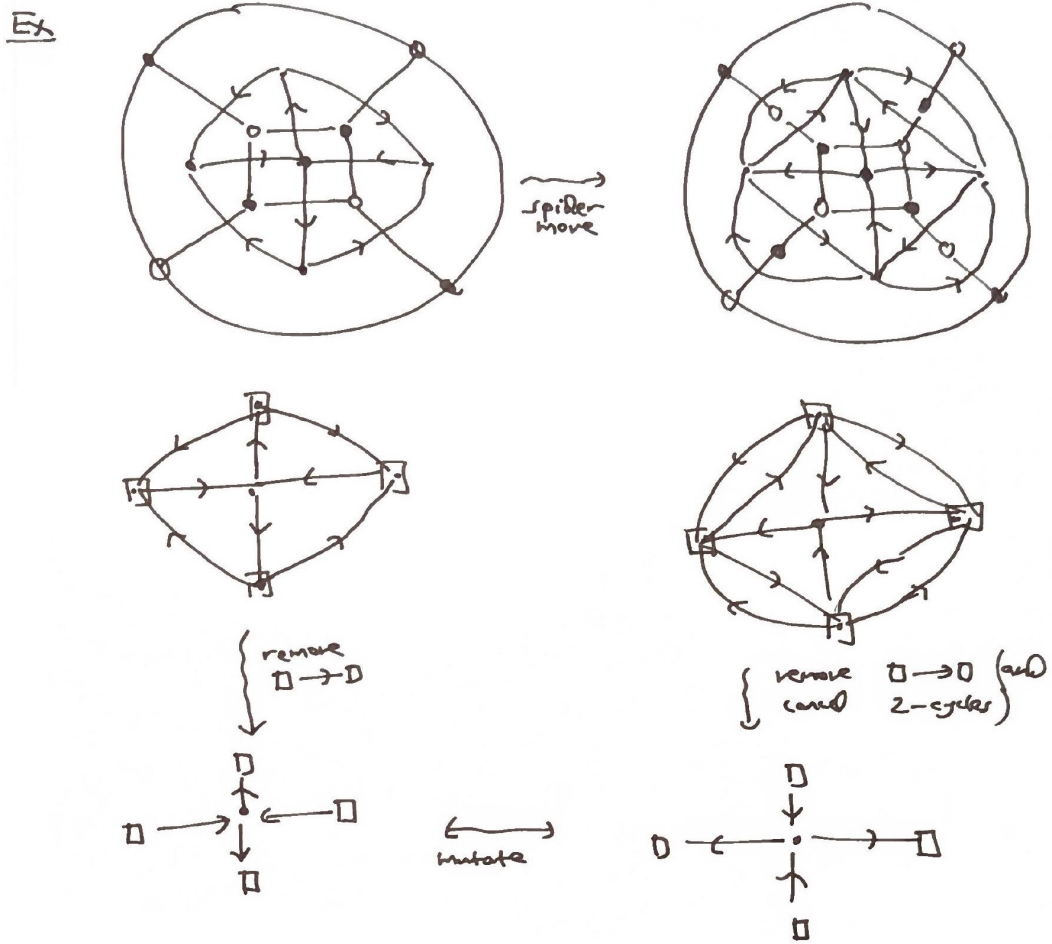


Figure 23: Two plabic graphs related by a spider move, and their quivers related by mutation.

The extended exchange matrix is

$$\tilde{B}(Q) = \begin{pmatrix} 0 & -1 & 1 \\ 1 & 0 & -1 \\ -1 & 1 & 0 \\ -1 & -1 & 0 \\ 2 & 0 & 0 \end{pmatrix}, \quad B(Q) = \begin{pmatrix} 0 & -1 & 1 \\ 1 & 0 & -1 \\ -1 & 1 & 0 \end{pmatrix}.$$

Example 5.3. Let Q be the Markov quiver. Figure 27 shows the extended exchange matrices for Q and two of its mutations.

Remark 5.4. Reordering the vertices of Q results in simultaneously reordering the rows $1, \dots, n$ and reordering the columns $1, \dots, m$.

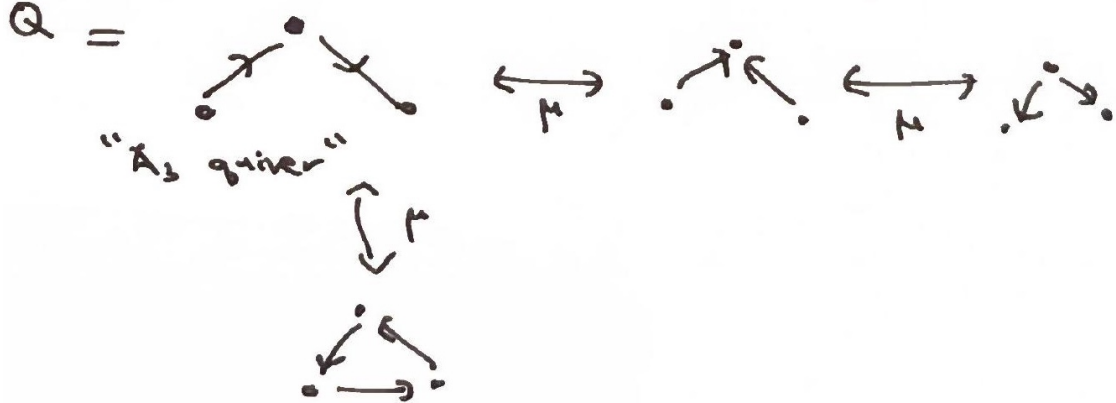


Figure 24: The mutation equivalence class of the A_3 quiver.



Figure 25: The Markov quiver.

5.2 Matrix Mutation

Lemma 5.5. For a quiver Q with $\tilde{B}(Q) = (b_{ij})$ and $Q' = \mu_k(Q)$ for a mutable vertex k of Q , we have $\tilde{B}(Q') = (b'_{ij})$ with

$$b'_{ij} = \begin{cases} -b_{ij} & \text{if } i = k \text{ or } j = k \\ b_{ij} + b_{ik}b_{kj} & \text{if } b_{ik}b_{kj} > 0 \\ b_{ij} - b_{ik}b_{kj} & \text{if } b_{ik}b_{kj} < 0 \\ b_{ij} & \text{else} \end{cases} \quad (*)$$

Note 5.6. One can replace the middle two cases with

$$b'_{ij} = b_{ij} + |b_{ik}|b_{kj} \quad \text{if } b_{ik}b_{kj} > 0.$$

Example 5.7. Figure 28 shows an example of matrix mutation.

5.3 Skew-Symmetrizable Matrices

Definition 5.8. An $n \times n$ matrix $B = (b_{ij}) \in \text{Mat}_{n \times n}(\mathbb{Z})$ is **skew-symmetrizable** if for some $d_1, \dots, d_n \in \mathbb{Z}_{>0}$ we have

$$d_i b_{ij} = -d_j b_{ji}.$$

(I.e., B becomes skew-symmetric after rescaling the rows by positive integers.)

Definition 5.9. An $m \times n$ matrix is **extended skew-symmetrizable** if the top $n \times n$ submatrix is skew-symmetrizable.

Definition 5.10. For $\tilde{B} = (b_{ij})$ an extended skew-symmetrizable $m \times n$ matrix and $k \in \{1, \dots, n\}$, we define $\mu_k(\tilde{B}) = (b'_{ij})$ using the same formula (*).

Figure 26: A quiver with frozen vertices 4 and 5 (boxed), and its extended and exchange matrices.

$$\tilde{\mathcal{B}}(Q) = \begin{pmatrix} 1 & 2 & 3 & 4 & 5 \\ 1 & 0 & -1 & 1 & 1 \\ 2 & 1 & 0 & -1 & 0 \\ 3 & -1 & 1 & 0 & 0 \\ 4 & -1 & -1 & 0 & 0 \\ 5 & 2 & 0 & 0 & 0 \end{pmatrix} \quad \mathcal{B}(Q) = \begin{pmatrix} 0 & -1 & 1 \\ 1 & 0 & -1 \\ -1 & 1 & 0 \end{pmatrix}$$

Figure 26: A quiver with frozen vertices 4 and 5 (boxed), and its extended and exchange matrices.

$E^+ : Q =$ 

 $\tilde{\mathcal{B}}(Q) = \begin{pmatrix} 0 & 2 & -2 \\ -2 & 0 & 2 \\ 2 & -2 & 0 \end{pmatrix}$



 $\tilde{\mathcal{B}}(Q) = \begin{pmatrix} 0 & -2 & 2 \\ 2 & 0 & -2 \\ -2 & 2 & 0 \end{pmatrix}$

Figure 27: The Markov quiver and extended exchange matrices for mutations.

Exercise 5.11. (1) $\mu_k(\tilde{B})$ is again extended skew-symmetrizable, using the same d_1, \dots, d_n .

- (2) $\mu_k(\mu_k(\tilde{B})) = \tilde{B}$.
- (3) $\mu_k(-\tilde{B}) = -\mu_k(\tilde{B})$.
- (4) If $b_{ij} = b_{ji} = 0$, then $\mu_i \mu_j \tilde{B} = \mu_j \mu_i \tilde{B}$.

5.4 Diagrams and Uniqueness

Definition 5.12. For a skew-symmetrizable $n \times n$ matrix $B = (b_{ij})$, its **diagram** is the weighted directed graph $\Gamma(B)$ with vertices $1, \dots, n$ and $i \rightarrow j$ if and only if $b_{ij} > 0$, with weight $|b_{ij}b_{ji}|$.

Lemma 5.13. If the diagram $\Gamma(B)$ of an $n \times n$ skew-symmetrizable matrix B is connected, then the skew-symmetrizing vector (d_1, \dots, d_n) is unique up to rescaling.

Proof. By connectedness, there is an ordering l_1, \dots, l_n of $\{1, \dots, n\}$ such that for each $j \geq 2$ we have $b_{l_i l_j} \neq 0$ for some $i < j$.

If (d_1, \dots, d_n) and (d'_1, \dots, d'_n) are skew-symmetrizing vectors, we have $d_i b_{ij} = -d_j b_{ji}$ and $d'_i b_{ij} = -d'_j b_{ji}$ for all i, j .

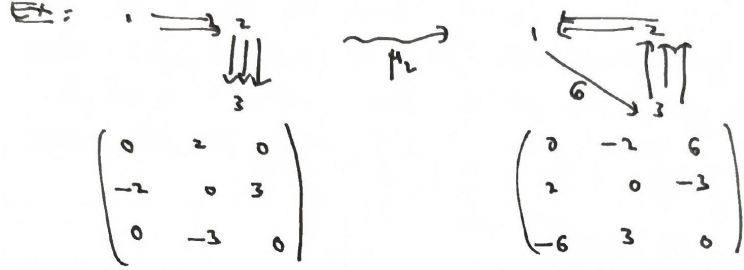


Figure 28: An example of quiver mutation μ_2 and the corresponding matrix mutation.

If $b_{ij} \neq 0$, we have

$$\frac{b_{ij}}{b_{ji}} = \frac{-d_j}{d_i} = \frac{-d'_j}{d'_i}.$$

Thus $\frac{d_j}{d'_j} = \frac{d_i}{d'_i}$. □

5.5 Mutation Equivalence for Matrices

Definition 5.14. Two extended skew-symmetrizable matrices \tilde{B}, \tilde{B}' are **mutation equivalent** if one can get from \tilde{B} to \tilde{B}' by a sequence of mutations followed by a reordering of the rows and columns in the sense from before. Put

$$[B] := \text{mutation equivalence class of } B.$$

Proposition 5.15. For an $n \times n$ skew-symmetrizable matrix, its rank and determinant are preserved by mutations.

Proof. One can write

$$b'_{ij} = \begin{cases} -b_{ij} & \text{if } k \in \{i, j\} \\ b_{ij} + \max(0, -b_{ik})b_{kj} + b_{ik} \max(0, b_{kj}) & \text{otherwise} \end{cases}$$

We have

$$\begin{aligned} \mu_k(B) &= J_{m,k} \tilde{B} J_{n,k} + J_{m,k} \tilde{B} F_k + E_k \tilde{B} J_{n,k} \\ &= (J_{m,k} + E_k) \tilde{B} (J_{n,k} + F_k) \end{aligned}$$

where:

- $J_{m,k}$ (resp. $J_{n,k}$) is a diagonal $m \times m$ (resp. $n \times n$) matrix with 1s on the diagonal except for -1 in the (k, k) entry.
- $E_k = (e_{ij})$ is an $m \times m$ matrix with $e_{ik} = \max(0, -b_{ik})$ and all other entries 0.
- $F_k = (f_{ij})$ is an $n \times n$ matrix with $f_{kj} = \max(0, b_{kj})$ and all other entries 0.

Note: $E_k \tilde{B} F_k = 0$ since $b_{kk} = 0$.

We have $\det(J_{m,k} + E_k) = \det(J_{n,k} + F_k) = -1$. □

5.6 Labeled Seeds

Definition 5.16. A **labeled seed of geometric type** in $\mathcal{F} = \mathbb{C}(x_1, \dots, x_m)$ (the field of rational functions) is a pair (\mathbf{x}, \tilde{B}) where:

- $\mathbf{x} = (x_1, \dots, x_m)$ is an m -tuple of elements of \mathcal{F} which form a free generating set (i.e., $\mathcal{F} = \mathbb{C}(x_1, \dots, x_m)$ and x_1, \dots, x_m are algebraically independent).
- $\tilde{B} = (b_{ij})$ is an $m \times n$ extended skew-symmetrizable matrix.

We say:

- \mathbf{x} is the (labeled) **extended cluster** of (\mathbf{x}, \tilde{B}) .
- (x_1, \dots, x_n) is the (labeled) **cluster**.
- x_1, \dots, x_n are the **cluster variables**.
- x_{n+1}, \dots, x_m are the **frozen variables**.
- \tilde{B} is the **extended exchange matrix**.
- Its top $n \times n$ submatrix B is the **exchange matrix**.

Example 5.17. Figure 29 shows two labeled seeds Σ and Σ' related by mutation, with $m = 3$ and $n = 2$.

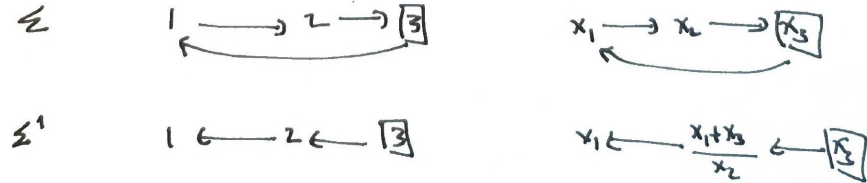


Figure 29: Two labeled seeds Σ and Σ' related by mutation at vertex 1.

For Σ : the extended cluster is $\mathbf{x} = (x_1, x_2, x_3)$, the cluster is (x_1, x_2) , the cluster variables are x_1, x_2 , the frozen variable is x_3 , and

$$\tilde{B} = \begin{pmatrix} 0 & 1 \\ -1 & 0 \\ 1 & -1 \end{pmatrix}, \quad B = \begin{pmatrix} 0 & 1 \\ -1 & 0 \end{pmatrix}.$$

For Σ' : the extended cluster is $\mathbf{x}' = (x'_1, \frac{x_1+x_3}{x_2}, x_3)$, the cluster variables are $x'_1, \frac{x_1+x_3}{x_2}$, and

$$\tilde{B}' = \begin{pmatrix} 0 & -1 \\ 1 & 0 \\ 0 & 1 \end{pmatrix}, \quad B' = \begin{pmatrix} 0 & -1 \\ 1 & 0 \end{pmatrix}.$$

6 Lecture 6

Date: February 4, 2026

Main reference: [FWZ21], §3.1.

6.1 Labeled Seeds and Seed Mutation

Recall: $\mathcal{F} = \mathbb{C}(y_1, \dots, y_m)$ is a field of rational functions, $m \geq n$. Say $x_1, \dots, x_m \in \mathcal{F}$ is a **free generating set** if it is algebraically independent and $\mathcal{F} = \mathbb{C}(x_1, \dots, x_m)$.

Definition 6.1. A **labeled seed** of geometric type in \mathcal{F} is (\tilde{x}, \tilde{B}) where:

- $\tilde{x} = (x_1, \dots, x_m)$ is a free generating set of \mathcal{F} .
- $\tilde{B} = (b_{ij})$ is an $m \times n$ extended skew-symmetrizable integer matrix.

Terminology:

- \tilde{x} is the **extended cluster**.
- $x = (x_1, \dots, x_n)$ is the **cluster**; x_1, \dots, x_n are the **cluster variables**.
- x_{n+1}, \dots, x_m are the **frozen variables**.
- \tilde{B} is the **extended exchange matrix**; the top $n \times n$ submatrix B is the **exchange matrix**.

Definition 6.2. Given (\tilde{x}, \tilde{B}) a labeled seed, $k \in \{1, \dots, n\}$, define a new labeled seed $\mu_k(\tilde{x}, \tilde{B}) = (\tilde{x}', \tilde{B}')$, where:

- $\tilde{B}' = \mu_k(\tilde{B})$
- $\tilde{x}' = (x'_1, \dots, x'_m)$, where $x'_j = x_j$ for $j \neq k$ and

$$x_k x'_k = \prod_{b_{ik} > 0} x_i^{b_{ik}} + \prod_{b_{ik} < 0} x_i^{-b_{ik}} \quad (\text{exchange relation})$$

Remark 6.3. When \tilde{B} comes from a quiver, the first product is over arrows ending at k and the second product is over arrows starting at k . See Figure 30 for an example.

6.2 Examples

Recall the Plücker relation (Figure 31):

$$P_{13}P_{24} = P_{12}P_{34} + P_{14}P_{23}.$$

More generally, a flip gives

$$P_{ik}P_{j\ell} = P_{ij}P_{\ell k} + P_{i\ell}P_{jk},$$

which is a special case of the exchange relation; see also Figure 32 for the wiring diagram case.

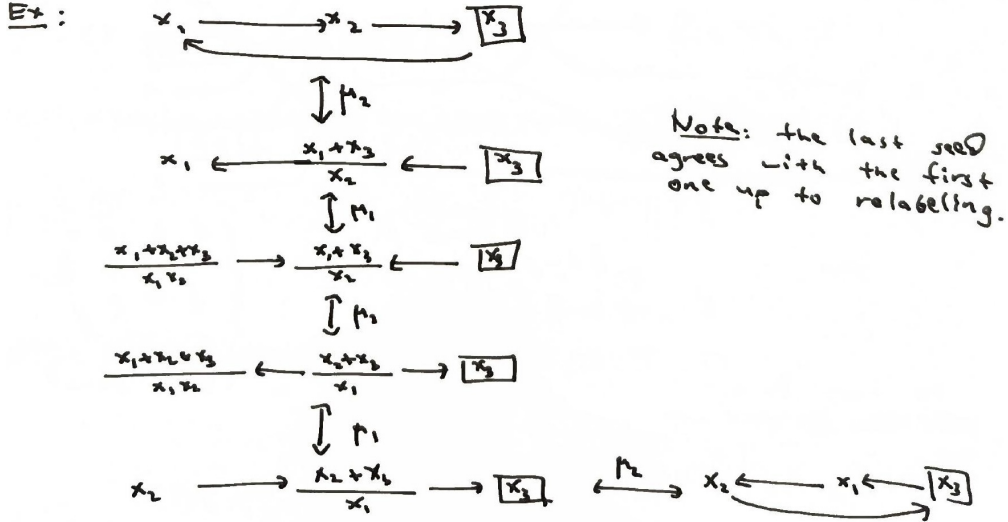


Figure 30: Example of a sequence of seed mutations. Note: the last seed agrees with the first one up to relabeling.

6.3 Seed Patterns and Cluster Algebras

Notation: Let \mathbb{T}_n denote the n -regular tree (Figure 33) with edges labeled by $1, \dots, n$, such that the edges incident to each vertex carry distinct labels.

Definition 6.4. A **seed pattern** is a choice of labeled seed $(\tilde{x}(t), \tilde{B}(t))$ for each vertex $t \in \mathbb{T}_n$, so that for each labeled edge $t \xrightarrow{k} t'$, the corresponding labeled seeds $(\tilde{x}(t), \tilde{B}(t))$ and $(\tilde{x}(t'), \tilde{B}(t'))$ differ by μ_k .

Note 6.5. A seed pattern is determined by any one of its seeds.

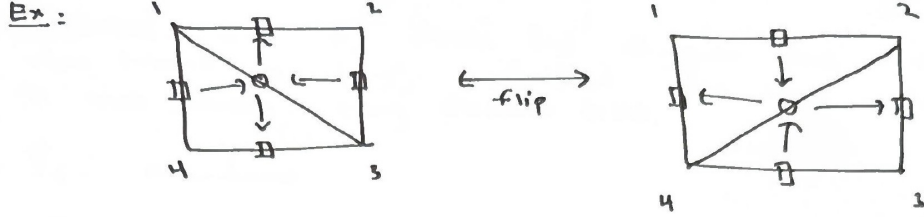
Definition 6.6. Let $(\tilde{x}(t), \tilde{B}(t))_{t \in \mathbb{T}_n}$ be a seed pattern, and put $R := \mathbb{C}[x_{n+1}, \dots, x_m]$. Let \mathcal{X} be the set of all cluster variables appearing in the seeds $x(t)$ for $t \in \mathbb{T}_n$. The **cluster algebra** \mathcal{A} is the R -subalgebra of \mathcal{F} generated by all cluster variables, i.e., $\mathcal{A} = R[\mathcal{X}]$.

Terminology: The **rank** n of any cluster is the rank of a cluster algebra.

Remark 6.7. Note that there is an isomorphism of \mathcal{F} mapping any free generating set to any other. In particular, up to isomorphism \mathcal{A} depends only on \tilde{B}_0 for any initial seed $(\tilde{x}_0, \tilde{B}_0)$, and in fact only on the mutation equivalence class of \tilde{B} . In particular, each (ice) quiver Q determines an extended exchange matrix \tilde{B} and hence a cluster algebra.

6.4 Examples of Cluster Algebras

- (1) **Triangulations:** The associated cluster algebra is the Plücker ring.
- (2) **Wiring diagrams:** For a wiring diagram, the associated cluster algebra is the algebra of regular functions on $\text{Flag}(\text{SL}_n)$ (i.e., on the Borel), generated by flag minors with the Plücker relations.
- (3) **Double wiring diagrams:** For a double wiring diagram, the associated cluster algebra is $\mathbb{C}[G]^U$ for $G = \text{SL}_n$, i.e., the ring of regular functions on the basic affine space.



$$\begin{pmatrix} a & b & c & d \\ e & f & g & h \end{pmatrix} \quad P_{13} = a_3 - c_2 \quad P_{24} = b_4 - d_1$$

Recall: $P_{13}P_{24} = P_{12}P_{34} + P_{14}P_{23}$

More generally,

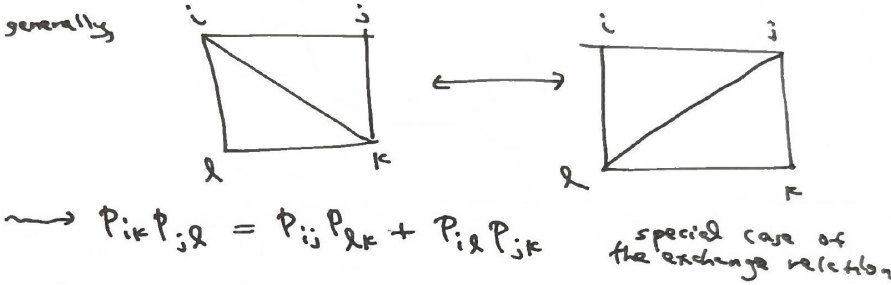


Figure 31: Triangulation flip and Plücker coordinates.

7 Lecture 7

Date: February 6, 2026

Main reference: [FWZ21], §3.2.

Recall: a labeled seed $(\tilde{x}_0, \tilde{B}_0)$ determines a seed pattern $(\tilde{x}(t), \tilde{B}(t))_{t \in \mathbb{T}_n}$, and hence a cluster algebra $\mathcal{A} \subset \mathcal{F}$ generated by all cluster variables and the frozen variables. Here $\tilde{x}_0 = (x_1, \dots, x_m)$ is a free generating set of $\mathcal{F} = \mathbb{C}(y_1, \dots, y_m)$, x_1, \dots, x_n are the cluster variables, x_{n+1}, \dots, x_m are the frozen variables, and the rank of \mathcal{A} is n .

7.1 Rank 1 Cluster Algebras

Example 7.1. (Rank $n = 1$.) The 1-regular tree is $\mathbb{T}_1 = \bullet - \bullet$. The extended exchange matrix is

$$\tilde{B}_0 = \begin{pmatrix} b_{21} \\ \vdots \\ b_{m1} \end{pmatrix}.$$

The exchange relation is

$$x_1 x'_1 = \prod_{b_{i1} > 0} x_i^{b_{i1}} + \prod_{b_{i1} < 0} x_i^{-b_{i1}} = M_1 + M_2,$$

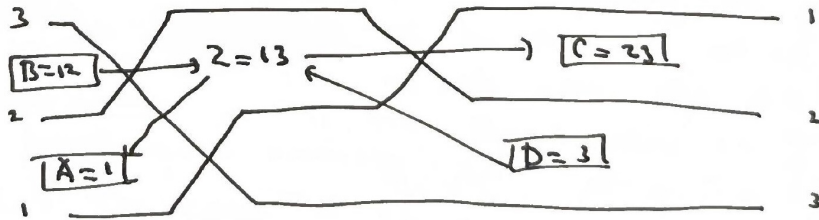
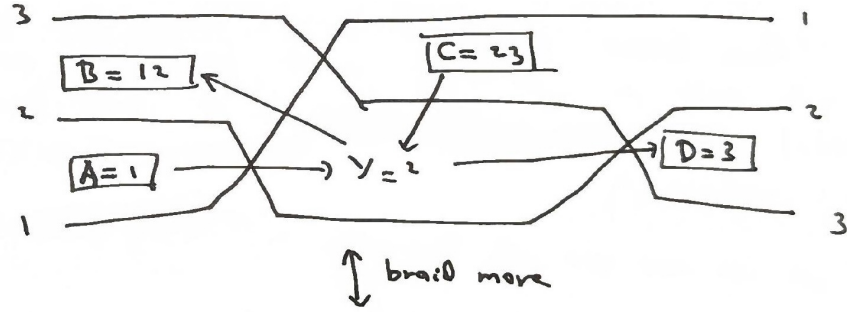
where M_1, M_2 are monomials in the frozen variables x_2, \dots, x_m . The cluster algebra is

$$\mathcal{A} = \mathbb{C}[x_1, x'_1, x_2, \dots, x_m] \subset \mathcal{F} = \mathbb{C}(x_1, x_2, \dots, x_m),$$

which has the presentation

$$\mathcal{A} \cong \mathbb{C}[z_1, z'_1, z_2, \dots, z_m] / (z_1 z'_1 = M_1 + M_2),$$

where M_1, M_2 are the corresponding monomials in z_2, \dots, z_m .



$$\begin{pmatrix} a & b & c \\ d & e & f \\ g & h & i \end{pmatrix}$$

$$\begin{aligned} A &\leftrightarrow a \\ B &\leftrightarrow ae-bd \\ C &\leftrightarrow bf-ce \end{aligned} \quad \text{etc}$$

$$\text{Have } Y_2 = AC + BD$$

special case of
the exchange relation

Figure 32: Wiring diagram braid move example. The relation $YZ = AC + BD$ is a special case of the exchange relation.

Example 7.2. Let $G = \mathrm{SL}_3(\mathbb{C})$ and let U be the subgroup of unipotent lower triangular 3×3 matrices. Then $\mathbb{C}[G]^U$ is a cluster algebra of rank 1.

Recall: $\mathbb{C}[G]^U$ is generated by flag minors P_J , $J \subsetneq \{1, 2, 3\}$. Here:

- $\mathcal{F} = \mathbb{C}(P_1, P_2, P_3, P_{12}, P_{23})$
- Frozen variables: P_1, P_3, P_{12}, P_{23}
- Cluster variables: P_2, P_{13}
- Single exchange relation: $P_2 P_{13} = P_1 P_{23} + P_3 P_{12}$

See Figure 34 for the corresponding wiring diagrams, where a braid move exchanges the cluster variables P_2 and P_{13} .

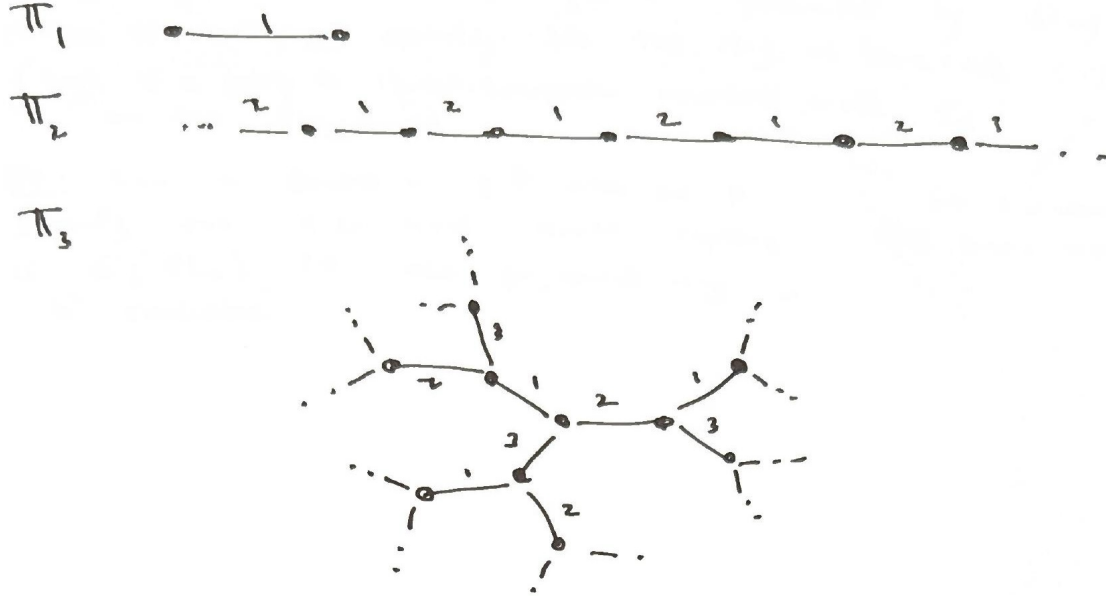


Figure 33: The n -regular trees \mathbb{T}_1 , \mathbb{T}_2 , and \mathbb{T}_3 .

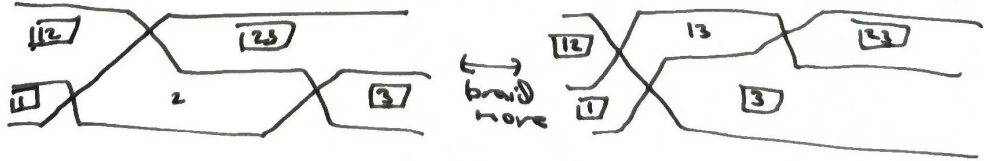


Figure 34: Wiring diagrams for SL_3 : the braid move exchanges the cluster variables P_2 and P_{13} , corresponding to the exchange relation $P_2P_{13} = P_1P_{23} + P_3P_{12}$.

7.2 Rank 2 Cluster Algebras

Example 7.3. (Rank $n = 2$.) The extended exchange matrix has the form

$$\tilde{B}_0 = \begin{pmatrix} 0 & \pm b \\ \mp c & 0 \\ b_{31} & b_{32} \\ \vdots & \vdots \\ b_{m1} & b_{m2} \end{pmatrix},$$

where either $b, c > 0$ or $b = c = 0$.

Suppose there are no frozens, i.e., $n = m$, so $\tilde{B}_0 = \begin{pmatrix} 0 & \pm b \\ \mp c & 0 \end{pmatrix}$. Then $\mu_1(\tilde{B}_0) = \mu_2(\tilde{B}_0) = -\tilde{B}_0$.

The exchange pattern along \mathbb{T}_2 has seeds

$$\cdots \xrightarrow{2} (z_1, z_0) \xrightarrow{1} (z_1, z_2) \xrightarrow{2} (z_3, z_2) \xrightarrow{1} (z_3, z_4) \xrightarrow{2} \cdots$$

with exchange matrices alternating between $\begin{pmatrix} 0 & b \\ -c & 0 \end{pmatrix}$ and $\begin{pmatrix} 0 & -b \\ c & 0 \end{pmatrix}$, and the exchange relation

gives

$$z_{k-1}z_{k+1} = \begin{cases} z_k^c + 1 & \text{if } k \text{ is even,} \\ z_k^b + 1 & \text{if } k \text{ is odd.} \end{cases}$$

Example 7.4. When $b = c = 0$, the extended exchange matrix is

$$\tilde{B} = \begin{pmatrix} 0 & 0 \\ 0 & 0 \\ b_{31} & b_{32} \\ \vdots & \vdots \\ b_{m1} & b_{m2} \end{pmatrix}.$$

Note that μ_k flips the sign of the k th column for $k = 1, 2$. The exchange relations are

$$x_1x'_1 = M_1 + M_2, \quad x_2x'_2 = M_3 + M_4,$$

where M_1, M_2, M_3, M_4 are monomials in the frozen variables. The cluster variables are x_1, x'_1, x_2, x'_2 , and this reduces to two rank 1 exchange patterns.

Notation: Let $\mathcal{A}(b, c)$ denote the cluster algebra of rank 2 with exchange matrices $\begin{pmatrix} 0 & \pm b \\ \mp c & 0 \end{pmatrix}$ and no frozen variables.

Example 7.5. $\mathcal{A}(1, 1)$: The exchange relation becomes $z_{k-1}z_{k+1} = z_k + 1$. We compute:

$$\begin{aligned} z_3 &= \frac{z_2 + 1}{z_1}, \\ z_4 &= \frac{z_3 + 1}{z_2} = \frac{z_1 + z_2 + 1}{z_1 z_2}, \\ z_5 &= \frac{z_4 + 1}{z_3}, \\ z_6 &= z_1, \quad z_7 = z_2, \quad \text{etc.} \end{aligned}$$

So the sequence of cluster variables is **5-periodic**.

Example 7.6. Consider $\tilde{B}_0 = \begin{pmatrix} 0 & 1 \\ -1 & 0 \\ p & q \end{pmatrix}$ with rank 2 and 1 frozen variable y , where $p, q \geq 0$ are integers. The seed pattern is:

$$\begin{array}{ccccccccc} (z_1, z_2) & \xrightarrow{1} & (z_3, z_2) & \xrightarrow{2} & (z_3, z_4) & \xrightarrow{1} & (z_5, z_4) & \xrightarrow{2} & (z_5, z_6) \\ \begin{pmatrix} 0 & 1 \\ -1 & 0 \\ p & q \end{pmatrix} & & \begin{pmatrix} 0 & -1 \\ 1 & 0 \\ -p & p+q \end{pmatrix} & & \begin{pmatrix} 0 & 1 \\ -1 & 0 \\ q & -(p+q) \end{pmatrix} & & \begin{pmatrix} 0 & -1 \\ 1 & 0 \\ -q & -p \end{pmatrix} & & \begin{pmatrix} 0 & 1 \\ -1 & 0 \\ -q & p \end{pmatrix} \end{array}$$

We have:

$$\begin{aligned} z_3 &= \frac{z_2 + y^p}{z_1}, \\ z_4 &= \frac{y^{p+q}z_1 + z_2 + y^p}{z_1 z_2}, \\ z_5 &= \frac{y^q z_1 + 1}{z_2}, \\ z_6 &= z_1, \quad z_7 = z_2, \quad \text{etc.} \end{aligned}$$

So the cluster variables are still **5-periodic**.

Remark 7.7. Although we assumed $p, q \geq 0$ above, up to mutating and swapping columns, every $(b, c) \in \mathbb{Z}^2$ can be written in one of the forms

$$(p, q), \quad (p+q, -p), \quad (q, -p-q), \quad (-p, -q), \quad (-q, p).$$

See Figure 35. Later we will view this as a simple example of a **scattering diagram**.

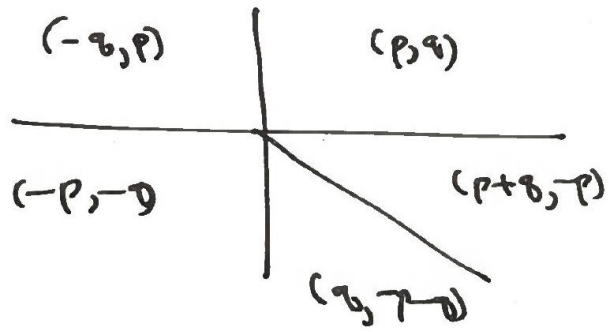


Figure 35: The five mutation forms of the frozen row (b, c) for a rank 2 cluster algebra with one frozen variable, viewed as a scattering diagram.

8 Lecture 8

Date: February 9, 2026

Main reference: [FWZ21], §3.3, §3.4.

8.1 Rank 2 examples (continued)

Example 8.1. $\mathcal{A}(1, 2)$: The exchange relation is

$$z_{k-1}z_{k+1} = \begin{cases} z_k^2 + 1 & \text{if } k \text{ is even,} \\ z_k + 1 & \text{if } k \text{ is odd.} \end{cases}$$

We compute:

$$\begin{aligned} z_3 &= \frac{z_2^2 + 1}{z_1}, \\ z_4 &= \frac{z_3 + 1}{z_2} = \frac{z_1 + z_2^2 + 1}{z_1 z_2}, \\ z_5 &= \frac{z_1^2 + 2z_1 + 1 + z_2^2}{z_1 z_2^2}, \\ z_6 &= \frac{z_1 + 1}{z_2}, \\ z_7 &= z_1, \quad z_8 = z_2, \quad \text{etc.} \end{aligned}$$

So the sequence of cluster variables is **6-periodic**.

Example 8.2. $\mathcal{A}(1, 3)$: The exchange relation is

$$z_{k-1}z_{k+1} = \begin{cases} z_k^3 + 1 & \text{if } k \text{ is even,} \\ z_k + 1 & \text{if } k \text{ is odd.} \end{cases}$$

Set $z_1 = z_2 = 1$. Then:

$$\begin{aligned} z_3 &= \frac{z_2^3 + 1}{z_1} = 2, \\ z_4 &= \frac{z_3 + 1}{z_2} = \frac{2 + 1}{1} = 3, \\ z_5 &= \frac{z_4^3 + 1}{z_3} = \frac{28}{2} = 14, \\ z_6 &= \frac{z_5 + 1}{z_4} = \frac{15}{3} = 5, \\ z_7 &= \frac{z_6^3 + 1}{z_5} = \frac{126}{14} = 9, \\ z_8 &= \frac{z_7 + 1}{z_6} = \frac{10}{5} = 2, \\ z_9 &= \frac{z_8^3 + 1}{z_7} = \frac{9}{9} = 1, \\ z_{10} &= \frac{z_9 + 1}{z_8} = \frac{2}{2} = 1. \end{aligned}$$

So it is **8-periodic** at least after specializing $z_1 = z_2 = 1$, and we claim that it is 8-periodic even without this specialization.

Example 8.3. $\mathcal{A}(1, 4)$: Setting $z_1 = z_2 = 1$ gives the sequence

$$1, 1, 2, 3, 41, 14, 937, 67, 21506, 321, \dots$$

This is *not* periodic. However, all terms are integers, and in fact each z_k is a **Laurent polynomial** in z_1, z_2 .

8.2 The Laurent phenomenon

Theorem 8.4 (Laurent phenomenon). *Let $(\tilde{x}_0, \tilde{B}_0)$ be a labeled seed, with $\tilde{x}_0 = (x_1, \dots, x_m)$, and associated cluster algebra \mathcal{A} . Every cluster variable of \mathcal{A} is a Laurent polynomial with integer coefficients in the variables x_1, \dots, x_m . Moreover, x_{n+1}, \dots, x_m do not appear in the denominators.*

Remark 8.5. Note that we can replace \tilde{x}_0 equally with any other extended cluster of \mathcal{A} .

Proof idea. Say $t_0 \in \mathbb{T}_n$ is the initial vertex with $(\tilde{x}_0, \tilde{B}_0)$ the initial (labeled) seed. Let $x = x(t)$ be a cluster variable in the seed at some vertex $t \in \mathbb{T}_n$, where $\tilde{x}_0 = (x_1, \dots, x_m)$. We want to show that x is a Laurent polynomial in x_1, \dots, x_m . We use induction on $d = \text{dist}(t, t_0)$.

Base cases:

- If $d = 1$, then $x(t_1) = (x_1, \dots, x'_j, \dots, x_m)$ where

$$x'_j = \frac{\prod_{b_{ij} > 0} x_i^{b_{ij}} + \prod_{b_{ij} < 0} x_i^{-b_{ij}}}{x_j},$$

which is already a Laurent polynomial.

- If $d = 2$, then $x(t_2) = (x_1, \dots, x'_j, \dots, x'_k, \dots, x_m)$ where

$$x'_k = \frac{\text{poly in } x_1, \dots, x'_j, \dots, x_m}{x_k} = \frac{\text{Laurent poly in } x_1, \dots, x_m}{x_k}$$

(or swap j and k).

Inductive step: Now assume $d \geq 3$, and assume for simplicity that $b_{jk}^0 = b_{kj}^0 = 0$ where $\tilde{B}_0 = (b_{ij}^0)$. (The case $b_{jk}^0 b_{kj}^0 < 0$ is more complicated.)

Put $t_3 := \mu_k(t_0)$ and $t_4 := \mu_j \mu_k(t_0)$. Consider the following portion of \mathbb{T}_n :

$$\begin{array}{ccccccc} & & k & & j & & \\ & & t_0 & - & t_3 & - & t_4 \\ j & | & & & & & \\ t_1 & -^k & t_2 & - & \dots & - & t \end{array}$$

Note: $\tilde{x}(t_4) = \tilde{x}(t_2)$, so both t_1, t_3 lie at distance $d - 1$ from a seed containing x . By induction:

$$x = \text{Laurent poly in } \tilde{x}(t_1) = \text{Laurent poly in } \tilde{x}(t_3).$$

Meanwhile, $x'_j = \frac{M_1 + M_2}{x_j}$ and $x'_k = \frac{M_3 + M_4}{x_k}$, for monomials M_1, M_2, M_3, M_4 in x_1, \dots, x_m .

Substituting:

$$x = \frac{\text{poly in } x_1, \dots, x_m}{(\text{monomial in } x_1, \dots, x_m) \cdot (M_1 + M_2)^a} = \frac{\text{poly in } x_1, \dots, x_m}{(\text{monomial in } x_1, \dots, x_m) \cdot (M_3 + M_4)^b}.$$

It suffices to show that $a = 0$.

Let \tilde{B}_0^{aug} be \tilde{B}_0 after adding an extra row of the form $(0, \dots, 1, \dots, 0)$ (with 1 in the j th entry).

Let \mathcal{A}_{aug} be the resulting cluster algebra with coefficient variables x_{n+1}, \dots, x_{m+1} .

Observe: an expression in \mathcal{A}_{aug} for x in terms of x_1, \dots, x_{m+1} specializes (setting $x_{m+1} = 1$) to an expression in \mathcal{A} for x in terms of x_1, \dots, x_m .

So x being a Laurent polynomial in x_1, \dots, x_m in \mathcal{A}_{aug} implies x is a Laurent polynomial in x_1, \dots, x_m in \mathcal{A} , hence WLOG we can assume \tilde{B}_0^{aug} instead of \tilde{B}_0 .

But then

$$x'_j = \frac{M_1^{\text{aug}} + M_2^{\text{aug}}}{x_j} = \frac{M_1 x_{m+1} + M_2}{x_j}, \quad x'_k = \frac{M_3^{\text{aug}} + M_4^{\text{aug}}}{x_k} = \frac{M_3 + M_4}{x_k}.$$

Then $M_1^{\text{aug}} + M_2^{\text{aug}}$ and $M_3 + M_4$ have no common factors (think about what happens if we specialize $x_1 = \dots = x_m = 1$), which implies $a = 0$. \square

8.3 Markov triples

Definition 8.6. A **Markov triple** is a triple $(a, b, c) \in \mathbb{Z}_{\geq 1}^3$ which satisfies the **Markov equation**:

$$a^2 + b^2 + c^2 = 3abc.$$

Example 8.7. $(1, 1, 1)$ is a Markov triple, and hence also its permutations. So is $(1, 2, 5)$ and its permutations: $(1, 5, 2), (2, 1, 5), (2, 5, 1), (5, 1, 2), (5, 2, 1)$.

Lemma 8.8. If (a, b, c) is a Markov triple, then so is (a, b, c') with $c' = \frac{a^2 + b^2}{c} = 3ab - c$.

Proof. Consider the equation $a^2 + b^2 + t^2 = 3abt$, i.e., $t^2 - 3abt + (a^2 + b^2) = 0$. If c is one root, the other one c' must satisfy $c + c' = 3ab$, i.e.,

$$c' = 3ab - c = \frac{3abc - c^2}{c} = \frac{a^2 + b^2}{c}.$$

This operation is called **Markov mutation**. \square

Lemma 8.9. If (a, b, c) is a Markov triple and $a \leq b < c$, then $c' = 3ab - c < c$.

Proof. Put $f(t) = t^2 - 3abt + (a^2 + b^2)$. Then

$$f(b) = b^2 - 3ab^2 + a^2 + b^2 = b^2(2 - 3a) + a^2 \leq -b^2 + a^2 \leq 0.$$

Then c' , the other root of f , must satisfy $c' \leq b < c$. \square

Corollary 8.10. Every Markov triple can be connected to $(1, 1, 1)$ by a sequence of Markov mutations.

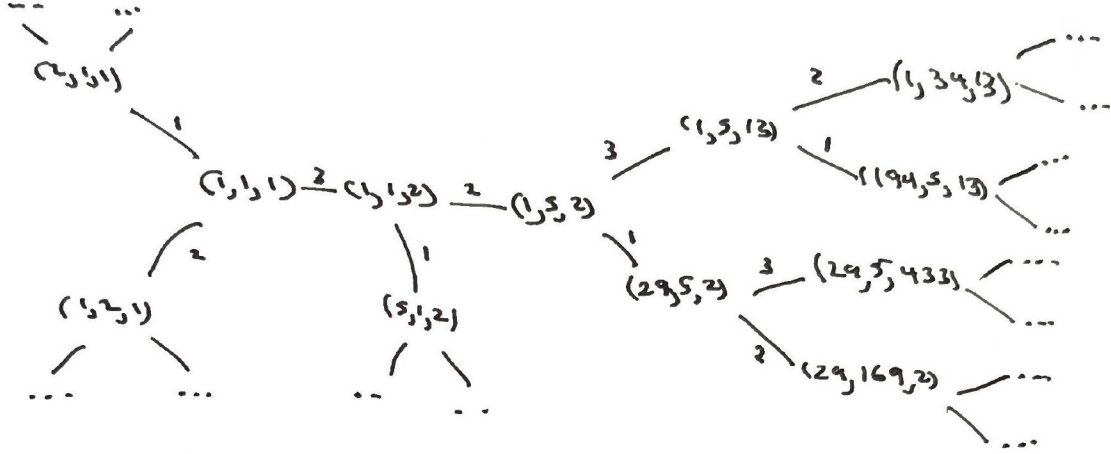


Figure 36: The Markov tree: nodes are Markov triples and edges correspond to Markov mutations.

8.4 The Markov tree

The Markov triples are organized into the **Markov tree**, where the edges correspond to Markov mutations (see Figure 36). Each edge is labeled by the index (1, 2, or 3) of the entry being mutated. For example:

$$(1, 1, 1) \xrightarrow{3} (1, 1, 2) \xrightarrow{2} (1, 5, 2) \xrightarrow{3} (1, 5, 13) \xrightarrow{1} (194, 5, 13), \dots$$

Recall: the **Markov quiver** is the quiver on three vertices with exchange relations (see Figure 37):

$$\begin{aligned} x'_1 x_1 &= x_2^2 + x_3^2, \\ x'_2 x_2 &= x_1^2 + x_3^2, \\ x'_3 x_3 &= x_1^2 + x_2^2. \end{aligned}$$

Thus for any cluster $\tilde{x} = (x_1, x_2, x_3)$, specializing the initial cluster variables to $(1, 1, 1)$ turns the trio into a Markov triple.

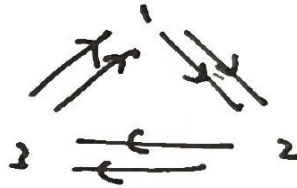


Figure 37: The Markov quiver: three vertices with double arrows forming a cycle.

8.5 The Somos-4 sequence

Example 8.11. The **Somos-4 sequence** is defined by $z_0 = z_1 = z_2 = z_3 = 1$ and the recurrence

$$\tilde{z}_{m+2} \tilde{z}_{m-2} = \tilde{z}_{m+1} \tilde{z}_{m-1} + \tilde{z}_m^2,$$

i.e., the sequence

$$1, 1, 1, 1, 2, 3, 7, 23, 59, 314, 1529, \dots$$

Somos (1980s): these are all integers!

To explain this using cluster algebras, consider the quiver Q on four vertices with no frozen variables shown in Figure 38. The exchange relation at vertex 1 is

$$z_1 z_5 = z_2 z_4 + z_3^2, \quad Q' = \mu_1(Q).$$

Then μ_1 rotates Q by $\pi/2$. Applying μ_2 to Q' gives

$$z_2 z_6 = z_3 z_5 + z_4^2.$$

Continuing in this way with the mutation sequence $\mu_1, \mu_2, \mu_3, \mu_4, \mu_1, \mu_2, \mu_3, \mu_4, \dots$ gives

$$\tilde{z}_n = \text{Laurent polynomial in } z_1, z_2, z_3, z_4.$$

Specializing $z_1 = z_2 = z_3 = z_4 = 1$, the k th element of Somos-4 is necessarily an integer by the Laurent phenomenon.

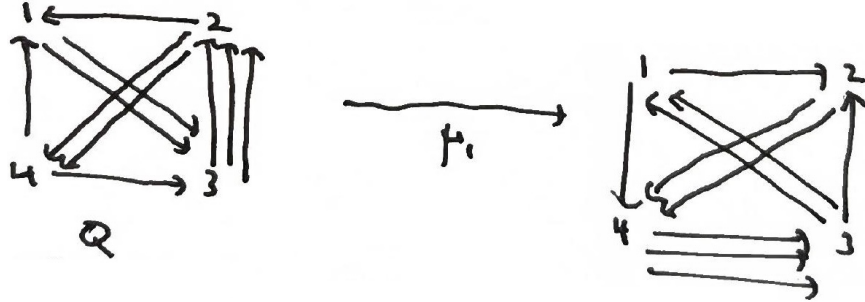


Figure 38: The quiver Q for the Somos-4 sequence (left) and its mutation $\mu_1(Q)$ (right), which is Q rotated by $\pi/2$.

9 Lecture 9

Date: February 11, 2026

Main reference: [FWZ21], §3.4, §3.5, §3.6.

9.1 The \hat{y} -variables

Let (\tilde{x}, \tilde{B}) be a labeled seed, with $\tilde{x} = (x_1, \dots, x_m)$, $\tilde{B} = (b_{ij})$. Put $(\tilde{x}', \tilde{B}') = \mu_k(\tilde{x}, \tilde{B})$, with $\tilde{x}' = (x'_1, \dots, x'_m)$, $\tilde{B}' = (b'_{ij})$.

Put $\hat{y} := (\hat{y}_1, \dots, \hat{y}_n)$, where

$$\hat{y}_j = \prod_{i=1}^m x_i^{b_{ij}},$$

and similarly $\hat{y}' = (\hat{y}'_1, \dots, \hat{y}'_n)$ with $\hat{y}'_j = \prod_{i=1}^m (x'_i)^{b'_{ij}}$.

Proposition 9.1. *We have (for $j = 1, \dots, n$):*

$$\hat{y}'_j = \begin{cases} \hat{y}_k^{-1} & \text{if } j = k, \\ \hat{y}_j \left(\hat{y}_k^{-\operatorname{sgn}(b_{kj})} + 1 \right)^{-b_{kj}} & \text{else.} \end{cases}$$

$$\text{Here } \operatorname{sgn}(b) = \begin{cases} 1 & \text{if } b > 0, \\ -1 & \text{if } b < 0. \end{cases}$$

Remark 9.2. • Recall that the exchange relation is

$$x_k x'_k = \prod_{b_{ik} > 0} x_i^{b_{ik}} + \prod_{b_{ik} < 0} x_i^{-b_{ik}}.$$

Then \hat{y}_k is the ratio of these two monomials.

• The above formula for \hat{y}'_j depends only on the top $n \times n$ submatrix of \tilde{B} .

Proof of Proposition 9.1. Case $j = k$: We have

$$\hat{y}'_k = \prod_{i=1}^m (x'_i)^{b'_{ik}} = \prod_{i \neq k} x_i^{b'_{ik}}.$$

Recall the mutation formula:

$$b'_{ij} = \begin{cases} -b_{ij} & \text{if } k \in \{i, j\}, \\ b_{ij} + |b_{ik}|b_{kj} & \text{if } b_{ik}b_{kj} > 0, \\ b_{ij} & \text{else.} \end{cases}$$

Since $k \in \{i, k\}$, we have $b'_{ik} = -b_{ik}$, so

$$\hat{y}'_k = \prod_{i \neq k} x_i^{-b_{ik}} = \hat{y}_k^{-1}.$$

Case $j \neq k$ and $b_{kj} \leq 0$:

$$\begin{aligned}
\hat{y}'_j &= (x'_k)^{b'_{kj}} \prod_{i \neq k} x_i^{b'_{ij}} \\
&= (x'_k)^{-b_{kj}} \left(\prod_{i \neq k} x_i^{b_{ij}} \right) \left(\prod_{b_{ik} < 0} x_i^{-b_{ik}b_{kj}} \right) \\
&= x_k^{b_{kj}} \left(\prod_{b_{ik} > 0} x_i^{b_{ik}} + \prod_{b_{ik} < 0} x_i^{-b_{ik}} \right)^{-b_{kj}} \left(\prod_{i \neq k} x_i^{b_{ij}} \right) \left(\prod_{b_{ik} < 0} x_i^{-b_{ik}b_{kj}} \right) \\
&= \left(\prod_i x_i^{b_{ij}} \right) (\hat{y}_k + 1)^{-b_{kj}} \\
&= \hat{y}_j (\hat{y}_k + 1)^{-b_{kj}}.
\end{aligned}$$

The case $j \neq k, b_{kj} \geq 0$ is similar. \square

9.2 Y-seeds

Definition 9.3. A **Y-seed** of rank n in a field \mathcal{F} is a pair (Y, B) , where:

- $Y = (Y_1, \dots, Y_n)$ is an n -tuple of elements in \mathcal{F} ,
- B is a skew-symmetrizable $n \times n$ integer matrix.

We mutate Y-seeds as follows:

$$(Y, B) \xrightarrow{\mu_k} (Y', B'), \quad \text{where } B' = \mu_k(B),$$

$Y' = (Y'_1, \dots, Y'_n)$ with

$$Y'_j = \begin{cases} Y_k^{-1} & \text{if } j = k, \\ Y_j \left(Y_k^{-\text{sgn}(b_{kj})} + 1 \right)^{-b_{kj}} & \text{else.} \end{cases}$$

Thus a labeled seed (\tilde{x}, \tilde{B}) gives rise to a Y-seed (\hat{y}, B) , where B is the top $n \times n$ submatrix of \tilde{B} and $\hat{y} = (\hat{y}_1, \dots, \hat{y}_n)$ with $\hat{y}_i = \prod_{i=1}^m x_i^{b_{ij}}$.

Remark 9.4. The seed mutation at k leaves x_j alone for $j \neq k$ but potentially changes all of Y_1, \dots, Y_n . However, the formula for x'_k involves all of x_1, \dots, x_m , whereas the formula for Y'_j only involves Y_k and Y_j .

9.3 Semifields

Definition 9.5. A **semifield** is an abelian group \mathbb{P} (written multiplicatively) endowed with an auxiliary operation \oplus which is commutative, associative, and distributive with respect to the group operation on \mathbb{P} . Note that (\mathbb{P}, \oplus) is only a semigroup (i.e., not necessarily having an identity or inverses).

Example 9.6. The multiplicative group $\mathbb{Q}_{>0}$, with \oplus given by ordinary addition.

Definition 9.7. The **tropical semifield** $\text{Trop}(q_1, \dots, q_\ell)$ is defined by:

- the multiplicative group of Laurent monomials in q_1, \dots, q_ℓ ,
- the auxiliary addition (**tropical addition**):

$$\prod_{i=1}^{\ell} q_i^{a_i} \oplus \prod_{i=1}^{\ell} q_i^{b_i} = \prod_{i=1}^{\ell} q_i^{\min(a_i, b_i)}.$$

Check:

- Commutative: $\min(a_i, b_i) = \min(b_i, a_i)$.
- Associative: $\min(\min(a_i, b_i), c_i) = \min(a_i, \min(b_i, c_i))$.
- Distributive (i.e., $p(q \oplus r) = pq \oplus pr$): $\min(a_i, b_i) + c_i = \min(a_i + c_i, b_i + c_i)$.

9.4 Coefficient tuples and tropical Y-seed mutation

For a labeled seed (\tilde{x}, \tilde{B}) with $\tilde{x} = (x_1, \dots, x_n, x_{n+1}, \dots, x_m)$ (where x_{n+1}, \dots, x_m are the frozen variables), we associate the **coefficient tuple**

$$y = (y_1, \dots, y_n), \quad \text{where } y_j = \prod_{i=n+1}^m x_i^{b_{ij}} \in \text{Trop}(x_{n+1}, \dots, x_m)$$

for $j = 1, \dots, n$.

Note 9.8. $B = \text{top } n \times n$ submatrix of \tilde{B} . Together with the coefficient tuple y , we recover the extended exchange matrix \tilde{B} .

Proposition 9.9. Let $\tilde{B} = (b_{ij})$ be an extended skew-symmetrizable $m \times n$ matrix with coefficient tuple $y = (y_1, \dots, y_n)$, and $\tilde{B}' = (b'_{ij}) = \mu_k(\tilde{B})$ with coefficient tuple $y' = (y'_1, \dots, y'_n)$. Then

$$y'_j = \begin{cases} y_k^{-1} & \text{if } j = k, \\ y_j \left(y_k^{-\text{sgn}(b_{kj})} \oplus 1 \right)^{-b_{kj}} & \text{else.} \end{cases}$$

This is called **tropical Y-seed mutation**.

Definition 9.10. The **universal semifield** $\mathbb{Q}_{\text{sf}}(x_1, \dots, x_m)$ is

$$\left\{ \frac{P(x_1, \dots, x_m)}{Q(x_1, \dots, x_m)} \in \mathbb{Q}(x_1, \dots, x_m) \mid P, Q \text{ have positive coefficients} \right\}$$

with ordinary multiplication and addition.

Lemma 9.11. Given any semifield \mathbb{S} and elements $s_1, \dots, s_m \in \mathbb{S}$, there exists a unique semifield homomorphism $\mathbb{Q}_{\text{sf}}(x_1, \dots, x_m) \rightarrow \mathbb{S}$ sending $x_i \mapsto s_i$ for $i = 1, \dots, m$.

Proof of Proposition 9.9. Let $f: \mathbb{Q}_{\text{sf}}(x_1, \dots, x_m) \rightarrow \text{Trop}(x_{n+1}, \dots, x_m)$ be the semifield homomorphism sending

$$f(x_i) = \begin{cases} 1 & \text{if } i \leq n, \\ x_i & \text{if } i > n. \end{cases}$$

Note that f also sends x'_k to 1, since $x_k x'_k = M_1 + M_2$ implies

$$1 \cdot f(x'_k) = f(M_1) \oplus f(M_2) = 1$$

(since M_1, M_2 are monomials which share no frozen variables), so $f(x'_k) = 1$.

Also, $\hat{y}_j = \prod_{i=1}^m x_i^{b_{ij}}$ implies

$$f(\hat{y}_j) = \prod_{i=n+1}^m x_i^{b_{ij}} = y_j, \quad \text{for } j = 1, \dots, n,$$

and similarly $f(\hat{y}'_j) = y'_j$.

Thus, applying f to the formula from Proposition 9.1:

$$\hat{y}'_j = \begin{cases} \hat{y}_k^{-1} & \text{if } j = k, \\ \hat{y}_j \left(\hat{y}_k^{-\text{sgn}(b_{kj})} + 1 \right)^{-b_{kj}} & \text{else,} \end{cases}$$

gives

$$y'_j = \begin{cases} y_k^{-1} & \text{if } j = k, \\ y_j \left(y_k^{-\text{sgn}(b_{kj})} \oplus 1 \right)^{-b_{kj}} & \text{else.} \end{cases}$$

□

10 Lecture 10

Date: February 13, 2026

Main reference: [FWZ21], §3.5, §3.6, §5.1.

10.1 Alternative characterization of labeled seeds

We can now give an alternative characterization of labeled seeds and their mutations. Fix $\mathcal{F} = \mathbb{C}(b_1, \dots, b_m)$. A **labeled seed** is a triple $\Sigma = (x, y, B)$, where:

- **cluster** $x = (x_1, \dots, x_n) \in \mathcal{F}^n$ such that $x \cup \{b_{n+1}, \dots, b_m\}$ freely generates \mathcal{F} ,
- **exchange matrix** $B = \text{skew-symmetrizable integer matrix}$,
- **coefficient tuple** $y = (y_1, \dots, y_n)$, where y_j is a Laurent monomial in $\text{Trop}(b_{n+1}, \dots, b_m)$.

For a mutation

$$(x, y, B) \xrightarrow{\mu_k} (x', y', B'),$$

we have:

- $B' = \mu_k(B)$,
- y' is given by the tropical Y-seed mutation rule,
- $x' = (x \setminus \{x_k\}) \cup \{x'_k\}$, with

$$x_k x'_k = \frac{y_k}{y_k \oplus 1} \prod_{b_{ik} > 0} x_i^{b_{ik}} + \frac{1}{y_k \oplus 1} \prod_{b_{ik} < 0} x_i^{-b_{ik}}.$$

Key point: From this perspective, the complexity of the mutation process does not really grow with the number $m - n$ of frozen variables.

10.2 Example: A_2 revisited

Consider $B_0 = \begin{pmatrix} 0 & 1 \\ -1 & 0 \end{pmatrix}$. This gives a labeled seed pattern on the line:

$$\dots \xrightarrow{1} \Sigma(-1) \xrightarrow{2} \Sigma(0) \xrightarrow{1} \Sigma(1) \xrightarrow{2} \Sigma(2) \xrightarrow{1} \Sigma(3) \xrightarrow{2} \dots$$

Write $\Sigma(t) = (x(t), y(t), B(t))$. Then $B(t) = (-1)^t \begin{pmatrix} 0 & 1 \\ -1 & 0 \end{pmatrix}$.

The cluster variables $x(t) = (x_1(t), x_2(t))$ and coefficient tuples $y(t) = (y_1(t), y_2(t))$ are given by:

| t | $x_1(t)$ | $x_2(t)$ | $y_1(t)$ | $y_2(t)$ |
|-----|---|---|---|--------------------------------|
| 0 | x_1 | x_2 | y_1 | y_2 |
| 1 | $\frac{y_1 + x_2}{x_1(y_1 \oplus 1)}$ | x_2 | $\frac{1}{y_1}$ | $\frac{y_1 y_2}{y_1 \oplus 1}$ |
| 2 | $\frac{y_1 + x_2}{x_1(y_1 \oplus 1)}$ | $\frac{x_1 y_1 y_2 + y_1 + x_2}{(y_1 y_2 \oplus y_1 \oplus 1) x_1 x_2}$ | $\frac{y_2}{y_1 y_2 \oplus y_1 \oplus 1}$ | $\frac{y_1 \oplus 1}{y_1 y_2}$ |
| 3 | $\frac{x_1 y_2 + 1}{x_2(y_2 \oplus 1)}$ | $\frac{x_1 y_1 y_2 + y_1 + x_2}{(y_1 y_2 \oplus y_1 \oplus 1) x_1 x_2}$ | $\frac{y_1 y_2 \oplus y_1 \oplus 1}{y_2}$ | $\frac{1}{y_1(y_2 \oplus 1)}$ |
| 4 | $\frac{x_1 y_2 + 1}{x_2(y_2 \oplus 1)}$ | x_1 | $\frac{1}{y_2}$ | $y_1(y_2 \oplus 1)$ |
| 5 | x_2 | x_1 | y_2 | y_1 |

10.3 Finite type classification in rank 2

Theorem 10.1. *A seed pattern with initial labeled seed $\Sigma = (x, y, B)$ with $B = \pm \begin{pmatrix} 0 & b \\ -c & 0 \end{pmatrix}$, $b, c \in \mathbb{Z}_{\geq 1}$, is of finite type if and only if $bc \leq 3$.*

Compare:

Proposition 10.2. *For $b, c \in \mathbb{Z}_{\geq 1}$, the subgroup $W = \langle R_1, R_2 \rangle \subset \mathrm{GL}_2$ generated by the reflections*

$$R_1 = \begin{pmatrix} -1 & b \\ 0 & 1 \end{pmatrix}, \quad R_2 = \begin{pmatrix} 1 & 0 \\ c & -1 \end{pmatrix}$$

is finite if and only if $bc \leq 3$.

Proof. Since $R_1^2 = R_2^2 = \mathbb{I}$, W is finite if and only if $R_1 R_2$ has finite order. We compute:

$$R_1 R_2 = \begin{pmatrix} bc - 1 & -b \\ c & -1 \end{pmatrix}.$$

The characteristic equation is

$$\lambda^2 - (bc - 2)\lambda + 1 = 0,$$

giving

$$\lambda = \frac{bc - 2 \pm \sqrt{(bc - 2)^2 - 4}}{2}.$$

For $bc = 1, 2, 3$: the roots have order 3, 4, 6 respectively.

If $bc > 4$: the roots are real and not ± 1 , hence $R_1 R_2$ has infinite order.

If $bc = 4$:

$$(R_1 R_2)^k = \begin{pmatrix} 2k + 1 & -kb \\ kc & 1 - 2k \end{pmatrix},$$

which also has infinite order. \square

Proof of Theorem 10.1. One can check that in the case $B = \pm \begin{pmatrix} 0 & 1 \\ -c & 0 \end{pmatrix}$, the seed pattern has 5 seeds if $c = 1$, 6 seeds if $c = 2$, and 8 seeds if $c = 3$.

Now assume $bc \geq 4$. Consider the seed pattern $(\Sigma(t))_{t \in \mathbb{Z}}$ with $\Sigma(t) = (x(t), y(t), B(t))$. Label the cluster variables as a sequence z_t ($t \in \mathbb{Z}$), where at each mutation step the new cluster variable gets the next index. The exchange relations become:

$$z_{t-1}z_{t+1} = \begin{cases} z_t^c + 1 & t \text{ even,} \\ z_t^b + 1 & t \text{ odd.} \end{cases}$$

Let $\mathbb{U} = \{u^r \mid r \in \mathbb{R}\}$ be the semifield with

$$u^r \oplus u^s = u^{\max(r,s)}, \quad u^r \cdot u^s = u^{r+s}$$

(u a formal variable).

Aim: Construct a semifield homomorphism $\Psi: \mathcal{F} \rightarrow \mathbb{U}^1$ such that $\{\Psi(z_t) \mid t \in \mathbb{Z}\}$ is infinite.

Case $bc > 4$: Let $\lambda > 1$ be a real eigenvalue of $\begin{pmatrix} bc-1 & -b \\ c & -1 \end{pmatrix}$.

Put $\Psi(z_1) = u^c$, $\Psi(z_2) = u^{\lambda+1}$.

The exchange relations become:

$$\Psi(z_{t-1})\Psi(z_{t+1}) = \begin{cases} \Psi(z_t)^c \oplus 1 & t \text{ even,} \\ \Psi(z_t)^b \oplus 1 & t \text{ odd.} \end{cases}$$

Claim 10.3. $\Psi(z_{2k+1}) = u^{\lambda^k c}$ and $\Psi(z_{2k+2}) = u^{\lambda^k(\lambda+1)}$.

Use induction. Writing $\Psi(z_t) = u^{\alpha_t}$:

$$\begin{aligned} \alpha_{2k+3} &= c\alpha_{2k+2} - \alpha_{2k+1} = c \cdot \lambda^k(\lambda+1) - \lambda^k c = \lambda^k c(\lambda+1-1) = \lambda^{k+1} c. \\ \alpha_{2k+4} &= b\alpha_{2k+3} - \alpha_{2k+2} = b \cdot \lambda^{k+1} c - \lambda^k(\lambda+1) \\ &= \lambda^k(bc\lambda - \lambda - 1) \\ &= \lambda^k(\lambda^2 + \lambda) \quad (\text{using } \lambda^2 - (bc-2)\lambda + 1 = 0) \\ &= \lambda^{k+1}(\lambda+1). \end{aligned}$$

Since $\lambda > 1$, $\alpha_t \rightarrow \infty$, so $\{\Psi(z_t)\}$ is infinite.

Case $bc = 4$: Instead use $\Psi(z_1) = u$, $\Psi(z_2) = u^b$.

Claim 10.4. $\Psi(z_{2k+1}) = u^{2k+1}$ and $\Psi(z_{2k+2}) = u^{(k+1)b}$.

This also follows by induction. Since $\alpha_t \rightarrow \infty$, the seed pattern has infinitely many cluster variables. \square

¹Warning: \mathcal{F} is not quite the right domain - it should be $\mathbb{Q}_{\text{sf}}(z_1, z_2)$.

10.4 2-finiteness

Definition 10.5. A skew-symmetrizable matrix $B = (b_{ij})$ is **2-finite** if for any $B' = (b'_{ij})$ mutation equivalent to B , we have $|b'_{ij}b'_{ji}| \leq 3$ for all i, j .

Corollary 10.6. *Finite type seed pattern \implies every exchange matrix is 2-finite.*

Proof. If $B \sim B'$ with $|b'_{ij}b'_{ji}| \geq 4$ for some i, j , then by freezing all the cluster variables in that seed except for x_i, x_j , we are reduced to the rank 2 case. \square

Remark 10.7. It turns out the converse to the above corollary is also true!

11 Lecture 11

Date: February 18, 2026

Main reference: [FWZ21], §5.2.

11.1 Cartan matrices and Dynkin diagrams

Definition 11.1. A **symmetrizable generalized Cartan matrix** is a square integer matrix $A = (a_{ij})$ such that:

- all diagonal entries are 2,
- all off-diagonal entries are ≤ 0 ,
- DA is symmetric for some diagonal matrix D with positive entries.

Definition 11.2. A **Cartan matrix** is a symmetrizable generalized Cartan matrix such that DA is positive definite (i.e. has only > 0 eigenvalues, or equivalently > 0 principal minors).

Note 11.3. For a Cartan matrix A , we must have

$$\det \begin{pmatrix} 2 & a_{ij} \\ a_{ji} & 2 \end{pmatrix} = 4 - a_{ij}a_{ji} > 0 \quad \text{for all } i \neq j,$$

i.e. $a_{ij}a_{ji} \leq 3$. In particular, $|a_{ij}|, |a_{ji}| \in \{0, 1, 2, 3\}$.

Example 11.4. $A = \begin{pmatrix} 2 & -b \\ -c & 2 \end{pmatrix}$ for $b, c \in \mathbb{Z}_{\geq 0}$ is Cartan if and only if it is one of:

- $b = c = 0$,
- $b = c = 1$,
- $b = 1, c = 2$ or $b = 2, c = 1$,
- $b = 1, c = 3$ or $b = 3, c = 1$.

Note that these “match” our classification of rank 2 cluster algebras of finite type.

Definition 11.5. Given an $n \times n$ Cartan matrix A , its **Dynkin diagram** $\text{Dynk}(A)$ is the graph with vertices $1, \dots, n$, where for each $i \neq j$ we put:

- a double edge with an arrow from i to j if $a_{ij} = -1, a_{ji} = -2$,
- a triple edge with an arrow from i to j if $a_{ij} = -1, a_{ji} = -3$,
- a single edge between i and j if $a_{ij} = a_{ji} = -1$.

Example 11.6. $A = \begin{pmatrix} 2 & -2 & 0 \\ -1 & 2 & -1 \\ 0 & -1 & 2 \end{pmatrix}$. The Dynkin diagram $\text{Dynk}(A)$ is of type B_3 (see Figure 39).

Example 11.7. $A = \begin{pmatrix} 2 & -1 \\ -3 & 2 \end{pmatrix}$. The Dynkin diagram $\text{Dynk}(A)$ is of type G_2 (see Figure 40).

$$\text{Ex: } A = \begin{pmatrix} 2 & -2 & 0 \\ -1 & 2 & -1 \\ 0 & -1 & 2 \end{pmatrix} \rightsquigarrow \text{Dynkin}(A) = \begin{array}{c} \text{Diagram of } B_3 \end{array}$$

Figure 39: The Dynkin diagram of type B_3 .

$$\text{Ex: } A = \begin{pmatrix} 2 & -1 \\ -3 & 2 \end{pmatrix} \rightsquigarrow \text{Dynkin}(A) = \begin{array}{c} \text{Diagram of } G_2 \end{array}$$

Figure 40: The Dynkin diagram of type G_2 .

Note 11.8. The above Dynkin diagram conventions are unrelated to the fact that the quiver with 3 arrows between two vertices corresponds to the skew-symmetric matrix $\begin{pmatrix} 0 & 3 \\ -3 & 0 \end{pmatrix}$.

Definition 11.9. A Cartan matrix is **indecomposable** if its Dynkin diagram is connected. The **type** of A is its equivalence class up to simultaneous permutations of the rows and columns.

Note 11.10. Any Cartan matrix is equivalent to a block-diagonal matrix with indecomposable blocks which correspond to the connected components of the corresponding Dynkin diagram. The type of A is determined by the multiplicity of each type of connected Dynkin diagram appearing in such a decomposition.

Theorem 11.11 (Cartan–Killing). *The Dynkin diagrams of indecomposable Cartan matrices are as follows (see Figure 41):*

$$A_n \ (n \geq 1), \quad B_n \ (n \geq 2), \quad C_n \ (n \geq 3), \quad D_n \ (n \geq 4), \quad E_6, E_7, E_8, \quad F_4, \quad G_2.$$

11.2 Finite type classification

Definition 11.12. Given an $n \times n$ skew-symmetrizable integer matrix $B = (b_{ij})$, its **Cartan counterpart** $\text{Cart}(B)$ is the symmetrizable generalized Cartan matrix (a_{ij}) , also $n \times n$, defined by

$$a_{ij} = \begin{cases} 2 & \text{if } i = j, \\ -|b_{ij}| & \text{if } i \neq j. \end{cases}$$

Theorem 11.13. *A cluster algebra is of finite type if and only if its seed pattern contains an exchange matrix B such that $\text{Cart}(B)$ is a Cartan matrix.*

Theorem 11.14. *Suppose that B_1, B_2 are skew-symmetrizable integer matrices such that $\text{Cart}(B_1), \text{Cart}(B_2)$ are Cartan. Then $\text{Cart}(B_1), \text{Cart}(B_2)$ have the same type if and only if B_1 and B_2 are mutation equivalent.*

Recall: The classification of simple complex Lie algebras (or equivalently, compact simply connected Lie groups) is precisely:

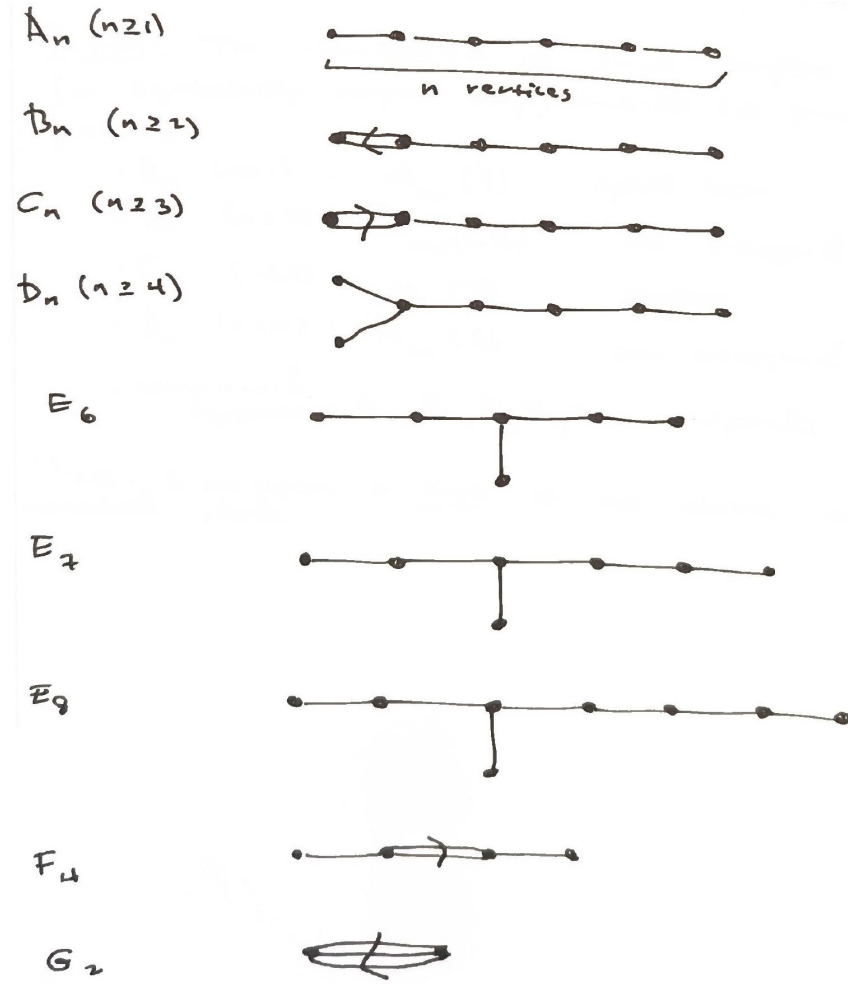


Figure 41: The Dynkin diagrams of indecomposable Cartan matrices (Theorem 11.11).

- A_n ($n \geq 1$): $\mathfrak{sl}_{n+1}(\mathbb{C})$ (special linear)
- B_n ($n \geq 2$): $\mathfrak{so}_{2n+1}(\mathbb{C})$ (odd orthogonal)
- C_n ($n \geq 3$): $\mathfrak{sp}_{2n}(\mathbb{C})$ (symplectic)
- D_n ($n \geq 4$): $\mathfrak{so}_{2n}(\mathbb{C})$ (even orthogonal)
- exceptional algebras: G_2, F_4, E_6, E_7, E_8 (sporadic)

Note 11.15. A Lie algebra is **simple** if it is not abelian and has no nontrivial ideals.

12 Lecture 12

Date: February 20, 2026

Main reference: [Wil14], Chapter 3.

12.1 Bordered surfaces with marked points

Definition 12.1. A **bordered surface with marked points** is a pair (S, M) , where

- S is an oriented connected surface, possibly with boundary,
- $M \subset S$ is a nonempty subset with at least one point on each boundary component.

We refer to elements of M as **marked points** and those in the interior of S as **punctures**.

For technical reasons, we will assume (S, M) is not a sphere with 1, 2, or 3 punctures, a monogon with 0 or 1 punctures, or a bigon or triangle without punctures (see Figure 42).

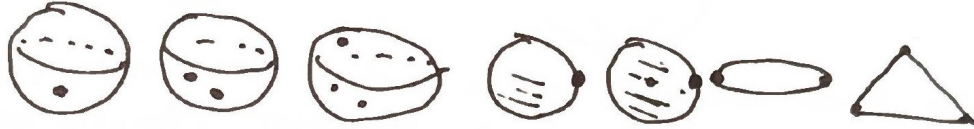


Figure 42: The excluded surfaces: spheres with 1, 2, or 3 punctures; monogons with 0 or 1 punctures; a bigon and triangle without punctures.

Definition 12.2. An **arc** σ in (S, M) is a curve in S (up to isotopy) such that:

- σ does not cross itself (except that its endpoints may coincide),
- apart from its endpoints, σ is disjoint from M and ∂S ,
- σ does not cut out an unpunctured monogon or an unpunctured bigon.

See Figure 43 for examples of valid and invalid arcs.

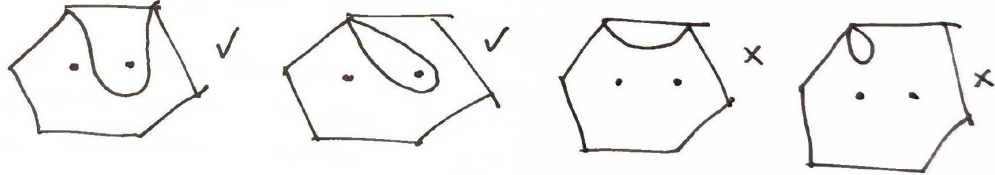


Figure 43: Examples of valid arcs (left) and invalid arcs (right).

Definition 12.3. A **boundary segment** is a curve which connects two marked points and lies entirely in ∂S without passing through a third marked point.

Definition 12.4. Two arcs are **compatible** if they have isotopic representatives which do not cross (except possibly at endpoints).

Definition 12.5. A **triangulation** is a maximal collection of pairwise compatible arcs, along with all boundary segments.

We refer to the components cut out by the arcs of a triangulation as “triangles.”

Note 12.6. Triangles may have either 3 distinct sides or only 2 (“self-folded”).

See Figure 44 for examples of triangulations, including a self-folded triangle.

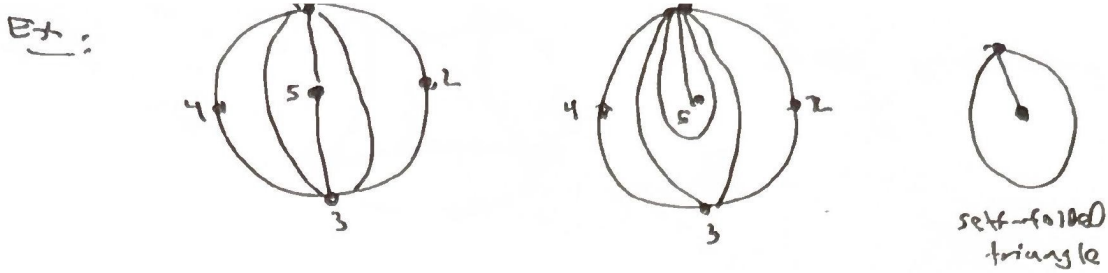


Figure 44: Examples of triangulations, including a self-folded triangle (right).

Definition 12.7. A **flip** of a triangulation T replaces a single arc σ by another arc $\sigma' \neq \sigma$ such that $T \setminus \{\sigma\} \cup \{\sigma'\}$ forms a new triangulation. The replacement arc σ' is unique if it exists.

Example 12.8. See Figure 45: we can flip along σ , but we cannot flip along η .

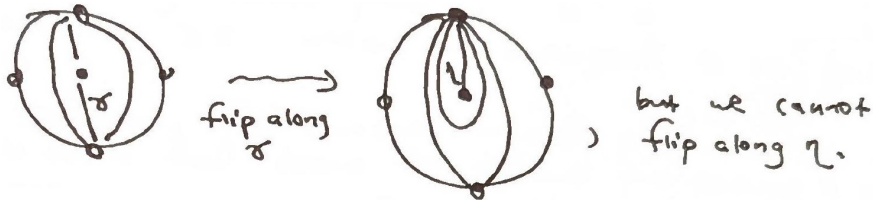


Figure 45: Flipping a triangulation along σ (left). The arc η cannot be flipped (right).

12.2 Teichmüller space and lambda lengths

Definition 12.9. Given a bordered surface S with marked points M , the (cusped) **Teichmüller space** $\mathcal{T}(S, M)$ is the space of all complete finite-area Riemannian metrics with constant curvature -1 on $S \setminus M$ and with geodesic boundary $\partial S \setminus M$, modulo $\text{Diff}_0(S, M)$.

Here $\text{Diff}_0(S, M)$ is the group of diffeomorphisms of S which fix M and are isotopic to the identity.

Note 12.10. There are cusps at the points of M , meaning they are infinitely far away, yet the total area is finite.

Recall: The **Poincaré disk model** for two-dimensional hyperbolic space is the open unit disk \mathbb{D} with the Riemannian metric

$$ds^2 = \frac{4(dx^2 + dy^2)}{(1 - x^2 - y^2)^2}$$

(constant curvature -1). The geodesics are of the form $C \cap \mathbb{D}$ for Euclidean circles $C \subset \mathbb{R}^2$ meeting $\partial\mathbb{D}$ orthogonally, and also $L \cap \mathbb{D}$ where $L \subset \mathbb{R}^2$ is a Euclidean line through the origin.

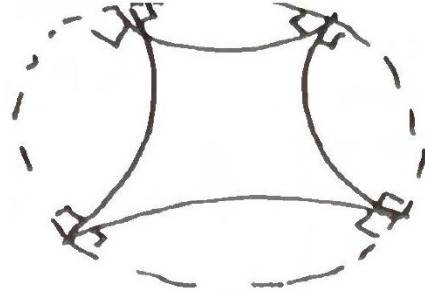


Figure 46: A hyperbolic quadrilateral in the Poincaré disk \mathbb{D} .

Example 12.11. Let P be a k -sided hyperbolic polygon cut out by geodesics in \mathbb{D} , equipped with the restriction of the hyperbolic metric (see Figure 46). This defines an element of $\mathcal{T}(S, M)$ with (S, M) having genus zero, one boundary component, and k boundary marked points.

Definition 12.12. Given $\Sigma \in \mathcal{T}(S, M)$, a **horocycle** around a puncture p is a closed curve in Σ which is orthogonal to all geodesics asymptotic to p . Similarly, a horocycle around a boundary marked point p is an arc joining two points of $\partial\Sigma$ which is orthogonal to all geodesics asymptotic to p .

Remark 12.13. Intuitively, the horocycle around p is the set of all points at a fixed distance from p , but this distance is infinite.

Example 12.14. The horocycles in \mathbb{D} are circles tangent to the boundary (see Figure 47).

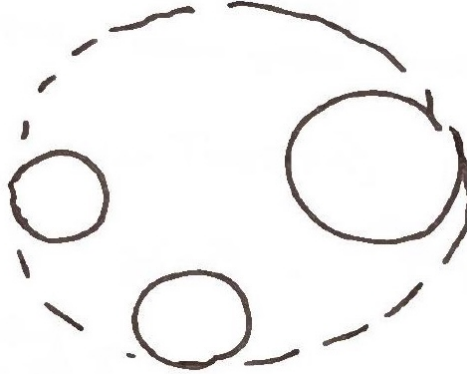


Figure 47: Horocycles in the Poincaré disk model are circles tangent to the boundary $\partial\mathbb{D}$.

Definition 12.15. The **decorated Teichmüller space** $\tilde{\mathcal{T}}(S, M)$ is defined similarly to $\mathcal{T}(S, M)$, but now we equip $S \setminus M$ with a collection of horocycles, one for each marked point in M .

Definition 12.16. Fix $\Sigma \in \tilde{\mathcal{T}}(S, M)$, and let σ be an arc or boundary segment in (S, M) . We define the **lambda length** $\lambda(\sigma)$ as follows. Let σ_Σ be the unique representative of σ which is geodesic with respect to the hyperbolic metric on Σ . Let $\ell(\sigma_\Sigma)$ be the signed distance along σ_Σ between the two horocycles at either end of σ_Σ , where the sign is positive if the two horocycles are disjoint and negative otherwise. Put

$$\lambda(\sigma) := \exp\left(\frac{\ell(\sigma_\Sigma)}{2}\right).$$

See Figure 48 for an illustration of a geodesic arc with horocycles at its endpoints.

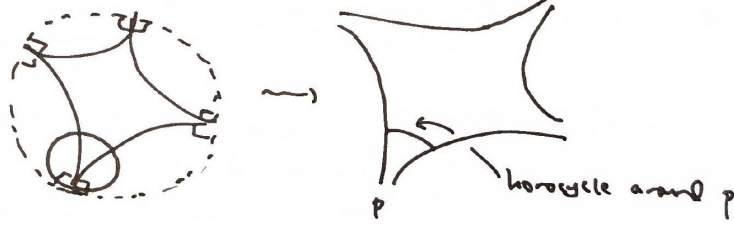


Figure 48: A geodesic arc with horocycles at its endpoints, illustrating the signed distance $\ell(\sigma_\Sigma)$.

Example 12.17. See Figure 49. In this example with 4 boundary marked points and no punctures, we have $\ell(\alpha_\Sigma), \ell(\beta_\Sigma), \ell(\delta_\Sigma) > 0$, but $\ell(\sigma_\Sigma) < 0$.

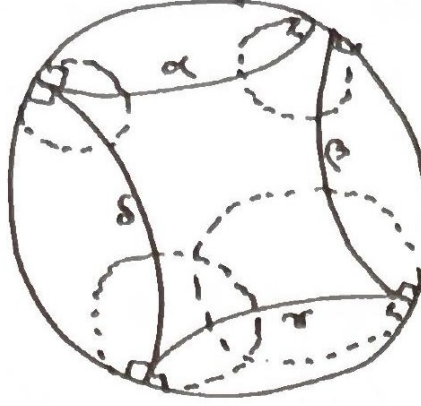


Figure 49: Lambda lengths on a quadrilateral: the signed distances $\ell(\alpha_\Sigma), \ell(\beta_\Sigma), \ell(\delta_\Sigma)$ are positive while $\ell(\sigma_\Sigma)$ is negative.

Note 12.18. We can depict a typical element $\Sigma \in \tilde{\mathcal{T}}(S, M)$ by a cartoon as in Figure 50. Note that such a picture is not in any way faithful to the hyperbolic metric on Σ ; in particular the boundary segments should be geodesic with respect to the hyperbolic metric.

Theorem 12.19 (Penner, Fomin–Thurston). *The map*

$$\prod_{\substack{\sigma \text{ arc or boundary} \\ \text{segment of } T}} \lambda(\sigma) : \tilde{\mathcal{T}}(S, M) \longrightarrow \mathbb{R}_{>0}^{n+c}$$

is a homeomorphism for any triangulation T . Here n denotes the number of arcs and c denotes the number of boundary marked points.

Remark 12.20. If S has genus g and b boundary components, and M consists of i interior marked points and c boundary marked points, one can compute the number n of arcs in any triangulation to be:

$$n = 6g + 3b + 3i + c - 6.$$

So

$$\dim \tilde{\mathcal{T}}(S, M) = 6g - 6 + 3b + 3i + 2c$$

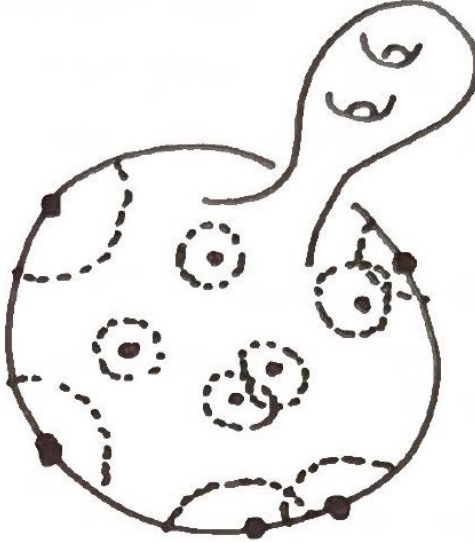


Figure 50: Cartoon depiction of an element $\Sigma \in \tilde{\mathcal{T}}(S, M)$ where S has genus two and one boundary component, and M consists of 5 boundary marked points and 5 punctures. Some of the horocycles intersect.

and

$$\dim \mathcal{T}(S, M) = \dim \tilde{\mathcal{T}}(S, M) - i - c = 6g - 6 + 3b + 2i + c,$$

the subtraction of $i + c$ being due to the choice of horocycles.

Proposition 12.21 (Hyperbolic Ptolemy). *Let $\alpha, \beta, \gamma, \delta$ be arcs or boundary segments which cut out a quadrilateral with diagonals η, θ . Then*

$$\lambda(\eta)\lambda(\theta) = \lambda(\alpha)\lambda(\gamma) + \lambda(\beta)\lambda(\delta),$$

where $\alpha, \beta, \gamma, \delta$ are ordered cyclically.

12.3 Exchange matrices from triangulations

We next associate an extended exchange matrix to any triangulation.

Definition 12.22. Let T be a triangulation of (S, M) with arcs τ_1, \dots, τ_n and boundary segments $\tau_{n+1}, \dots, \tau_{n+c}$. Put

$$\tilde{b}_{ij} = \#\{\text{triangles with sides } \tau_i, \tau_j \text{ in clockwise order}\} - \#\{\text{triangles with sides } \tau_i, \tau_j \text{ in counterclockwise order}\}.$$

The $(n + c) \times n$ **extended exchange matrix** of T is $\tilde{B}_T := (\tilde{b}_{ij})_{1 \leq i \leq n+c, 1 \leq j \leq n}$.

Remark 12.23. The above definition has to be modified if there are any self-folded triangles. Since every arc is a side of at most two triangles, we have $|\tilde{b}_{ij}| \leq 2$.

Proposition 12.24. *Flipping a triangulation T corresponds to mutating the associated extended exchange matrix \tilde{B}_T .*

Facts:

- Every arc in (S, M) is part of a triangulation.
- Any two triangulations differ by a sequence of flips.

Now let \mathcal{A} denote the cluster algebra associated to \tilde{B}_T . It follows that:

- each arc σ in (S, M) corresponds to a cluster variable $x_\sigma \in \mathcal{A}$,
- each triangulation T of (S, M) gives rise to a seed of \mathcal{A} .

Remark 12.25. There is an injective map

$$\{\text{arcs in } (S, M)\} \longrightarrow \{\text{cluster variables in } \mathcal{A}\},$$

but it is not generally surjective if there are any interior marked points, due to the fact that not all arcs can be flipped. There is a more general notion of “tagged arcs” and “tagged triangulations” which are in bijection with cluster variables and seeds respectively (due to Fomin–Shapiro–Thurston).

Remark 12.26. At least in the absence of punctures (i.e. interior marked points), we can view every element in \mathcal{A} as a function $\tilde{\mathcal{T}}(S, M) \rightarrow \mathbb{R}$. Are these “all of them” in any sense?

Even though not every seed corresponds to a triangulation (but rather a tagged triangulation), we still have:

Lemma 12.27. *For each seed of \mathcal{A} , the corresponding (extended) exchange matrix has all entries equal to 0, ± 1 , or ± 2 .*

Corollary 12.28. *For any (S, M) , the associated exchange matrix B is mutation-finite, i.e. only finitely many matrices appear in its mutation graph.*

12.4 Examples

Example 12.29. Consider the once-punctured torus (S, M) , i.e. $g = 1$, $b = 0$, $i = 1$, $c = 0$, and hence every triangulation has

$$n = 6g + 3b + 3i + c - 6 = 3 \quad \text{arcs.}$$

Figure 51 shows the beginning of the exchange graph. Using $H_1(\mathbb{T}^2) \cong \mathbb{Z}^2$, the arcs of the initial triangulation represent homology classes $\pm(1, 0)$, $\pm(0, 1)$, $\pm(1, 1)$.

Observe: If a triangulation has arcs with homology classes $\pm(a_1, b_1)$, $\pm(a_2, b_2)$, $\pm(a_3, b_3)$, then we must have

$$(a_3, b_3) = \pm(a_1 + a_2, b_1 + b_2) \quad \text{or} \quad (a_3, b_3) = \pm(a_1 - a_2, b_1 - b_2),$$

and μ_3 replaces one option with the other (and similarly for μ_1, μ_2).

Also, σ_1 and σ_2 intersect in $\left| \det \begin{pmatrix} a_1 & a_2 \\ b_1 & b_2 \end{pmatrix} \right| = |a_1b_2 - a_2b_1|$ points, so we must have $|a_1b_2 - a_2b_1| = 1$, and similarly $|a_1b_3 - a_3b_1| = |a_2b_3 - a_3b_2| = 1$.

Upshot: The exchange graph is dual to the **Farey tessellation** (see Figure 52): p/q and p'/q' are connected by an arc if and only if $|pq' - p'q| = 1$.

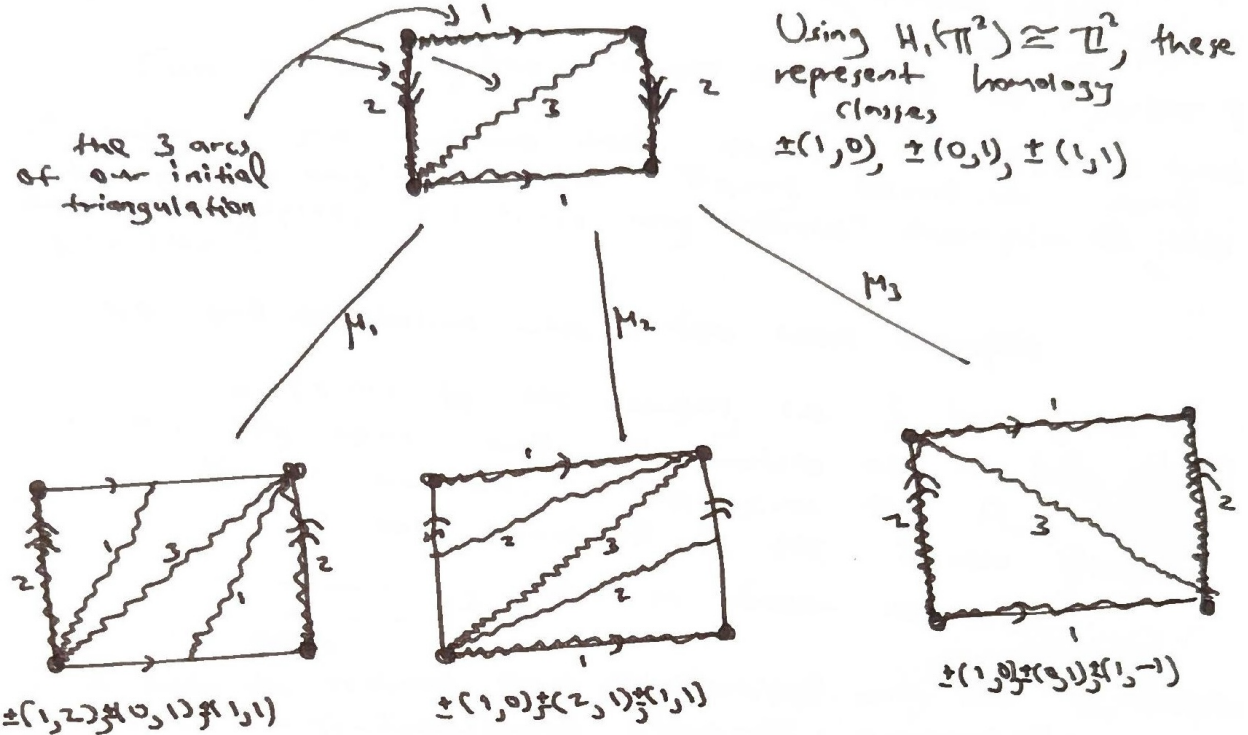


Figure 51: The beginning of the exchange graph for the once-punctured torus. Each triangulation has 3 arcs whose homology classes are shown.

Observe: For the triangulation T of the once-punctured torus, the corresponding exchange matrix is

$$\tilde{B}_T = \begin{pmatrix} 0 & -2 & 2 \\ 2 & 0 & -2 \\ -2 & 2 & 0 \end{pmatrix}$$

(no frozens). Reversing the orientation on \mathbb{T}^2 would flip these signs. This is exactly the exchange matrix of the Markov quiver!

Question 12.30. It follows that there is a bijective correspondence between triangles in the Farey tessellation and Markov triples. Is there any “direct” description of this bijection?

We end this lecture with a few more examples.

Example 12.31. Let (S, M) be the m -gon, i.e. S has genus 0 and one boundary component, and M consists of m boundary marked points and no punctures. This gives the A_{m-3} cluster algebra, i.e. the one associated to the Dynkin diagram

$$\underbrace{\bullet - \bullet - \bullet - \cdots - \bullet}_{m-3 \text{ vertices}},$$

plus m frozen variables. Recall that the exchange graph is identified with the 1-skeleton of the $(m-3)$ -dimensional Stasheff associahedron. Note that the number of cluster variables is exactly $\binom{m}{2} - m = \frac{m(m-3)}{2}$, and in particular is finite.

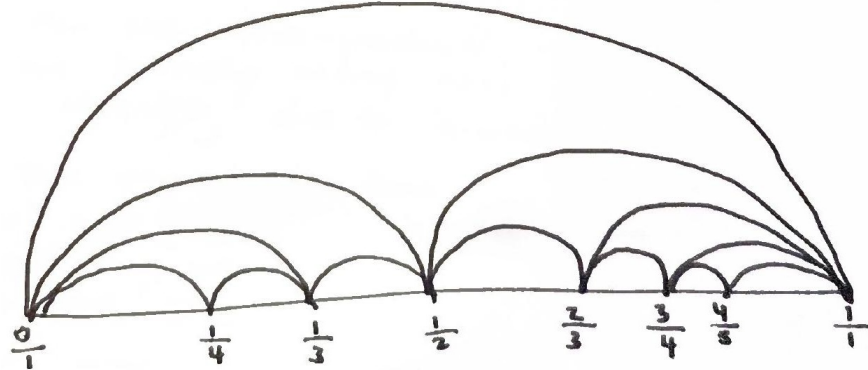


Figure 52: The Farey tessellation. Fractions p/q and p'/q' are connected by an arc if and only if $|pq' - p'q| = 1$.

Example 12.32. Let (S, M) be the once-punctured m -gon. This is the cluster algebra associated with the D_m Dynkin diagram. Note that there are only finitely many arcs, but this does not a priori imply only finitely many cluster variables.

Example 12.33. For the twice-punctured m -gon, it is easy to see that there are infinitely many arcs, and hence infinitely many cluster variables, due to braiding phenomena.

See Figure 53 for illustrations of the once-punctured and twice-punctured m -gons.



Figure 53: The once-punctured m -gon (top, giving D_m type) and the twice-punctured m -gon (bottom, with infinitely many arcs due to braiding).

Remark 12.34. One way to prove that $\{\text{arcs}\} \rightarrow \{\text{cluster variables}\}$ is injective is using hyperbolic Ptolemy and the fact that lambda lengths give a homeomorphism $\mathcal{T}(S, M) \cong \mathbb{R}_{>0}^{n+c}$.

Another way is as follows. For any arc σ , the cluster variable x_σ is a Laurent polynomial in the initial (extended) cluster variables x_1, \dots, x_m . Writing

$$x_\sigma = \frac{P_\sigma(x_1, \dots, x_m)}{x_1^{d_1} x_2^{d_2} \cdots x_m^{d_m}},$$

it turns out that the denominator vector (d_1, \dots, d_m) precisely records the intersection numbers of σ with the curves $\sigma_1, \dots, \sigma_m$ of the initial triangulation. Moreover, for distinct arcs σ_1, σ_2 , these intersection numbers cannot all be the same, i.e. $x_{\sigma_1} \neq x_{\sigma_2}$.

Remark 12.35. Here “intersection number” means interior intersections, i.e. σ intersects any boundary segment trivially. This is consistent with the fact that, when writing a cluster variable

as a Laurent polynomial in the extended cluster variables of a seed, the frozen variables do not appear in the denominators.

13 Lecture 13

Date: February 25, 2026

Main references: [Wil14], §3; [War14].

13.1 More examples of cluster algebras from surfaces

Example 13.1. Consider the bordered marked surface (S, M) with $g = 0$, $b = 2$, $i = 0$, $c = 2$. Then

$$n = 6g + 3b + 3i + c - 6 = 2,$$

i.e. every triangulation has 2 arcs. Choose a triangulation with arcs τ_1, τ_2 and boundary segments τ_3, τ_4 , with marked points M_1, M_2 (see Figure 54).

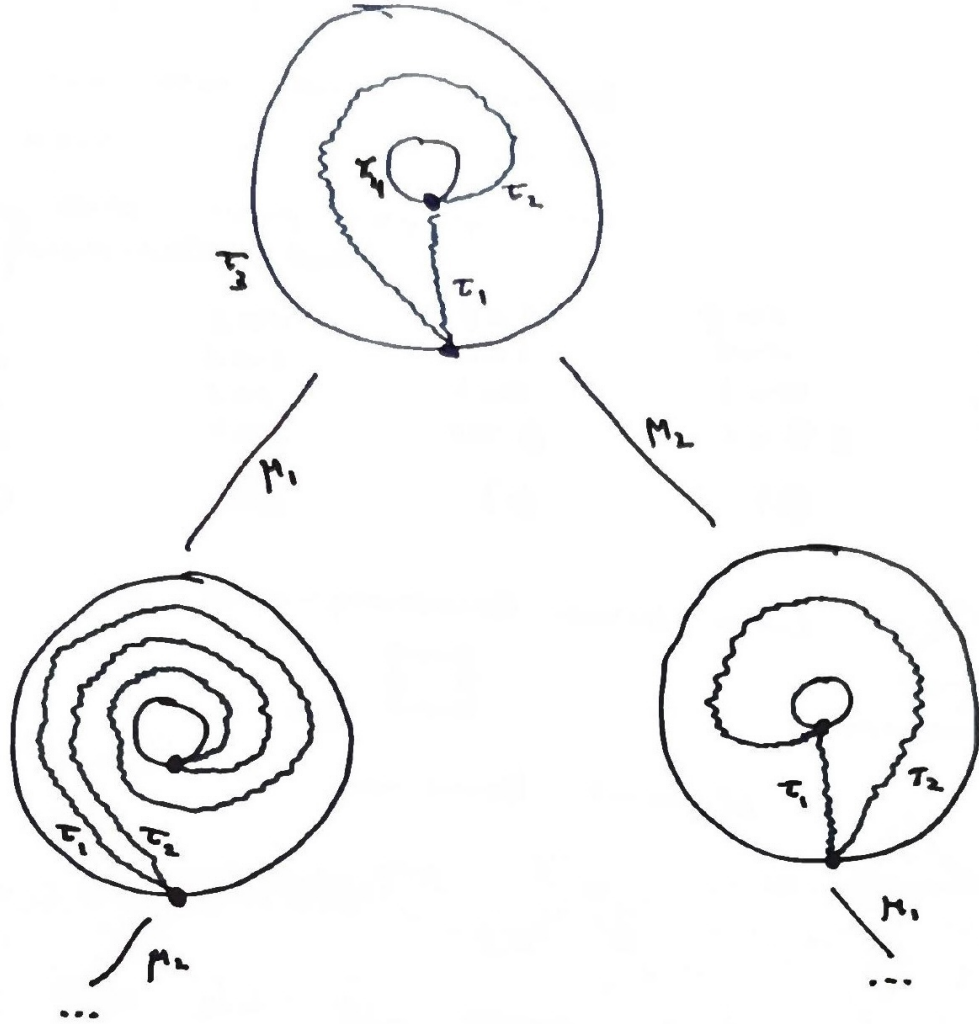
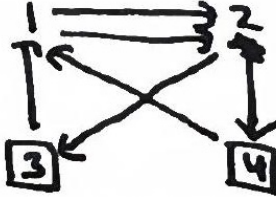


Figure 54: An annulus with one marked point on each boundary component. The initial triangulation (top) has arcs τ_1, τ_2 and boundary segments τ_3, τ_4 . Two alternative triangulations obtained by mutations μ_1 (left) and μ_2 (right) are shown below.

The initial triangulation has two triangles (see Figure 55). The corresponding quiver is shown below:



i.e. two arrows between vertices 1 and 2, plus two frozen vertices. This is the rank 2 cluster algebra $\mathcal{A}(2, 2)$ (plus 2冻子), with exchange graph a bi-infinite line and cluster variables

$$\dots, z_{-1}, z_0, z_1, z_2, z_3, \dots$$

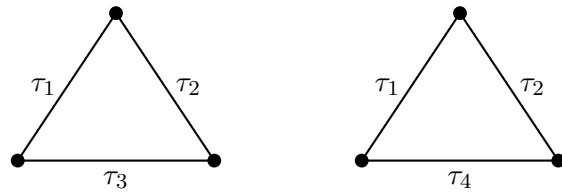


Figure 55: The two triangles of the initial triangulation, with sides τ_1, τ_2, τ_3 and τ_1, τ_2, τ_4 . The corresponding quiver is $1 \rightrightarrows 2$ with冻子 $\boxed{3}$ and $\boxed{4}$.

Example 13.2. The m -Kronecker quiver $1 \xrightarrow{m} 2$ for $m \geq 3$ is *not* surface-type.

Example 13.3. Consider the A_3 quiver (a 3-cycle). A single mutation transforms this into a linear quiver (see Figure 56). This is the A_3 cluster algebra, which corresponds to the hexagon.

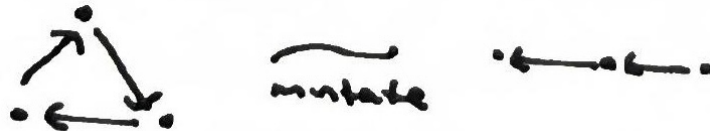


Figure 56: A mutation in the A_3 cluster algebra, which corresponds to the hexagon.

The number of triangulations of an m -gon is the Catalan number

$$C_{m-2} = \frac{1}{m-1} \binom{2m-4}{m-2}.$$

For small values:

| m | 3 | 4 | 5 | 6 | 7 |
|-----------|---|---|---|----|----|
| C_{m-2} | 1 | 2 | 5 | 14 | 42 |

The number of unlabeled seeds of A_{m-3} is also C_{m-2} , while the number of labeled seeds is $(m-3)! \cdot C_{m-2}$.



Figure 57: Mutating this acyclic quiver with 3 arrows produces one with 4 arrows.

13.2 Rank 3 surface-type cluster algebras

Example 13.4. The 3-point quiver (single arrows) mutates to a 3-cycle with the reversed orientation (see Figure 57).

Question 13.5. Does this come from a surface?

We would need $n = 6g + 3b + 3i + c - 6 = 3$. Recalling that every boundary component must have at least one marked point, the possibilities are:

| | (a) | (b) | (c) | (d) |
|-----|-----|-----|-----|-----|
| g | 1 | 0 | 0 | 0 |
| b | 0 | 1 | 1 | 2 |
| i | 1 | 1 | 0 | 0 |
| c | 0 | 3 | 6 | 3 |

(Note that we explicitly excluded the thrice-punctured sphere at the outset.)

Case (a): The once-punctured torus. This gives rise to the Markov cluster algebra, with the Markov quiver (a 3-cycle with 2 arrows on each edge); see Figure 58.

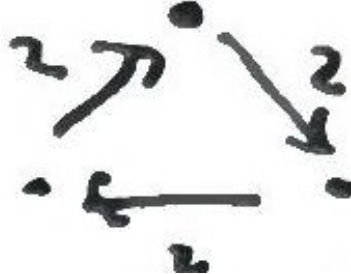


Figure 58: Case (a): the once-punctured torus gives the Markov cluster algebra, with the Markov quiver (a 3-cycle with 2 arrows on each edge).

Case (b): The once-punctured triangle. A triangulation and its corresponding quiver are shown in Figure 59. This gives the A_3 cluster algebra.

Note 13.6. In general, the once-punctured m -gon gives D_m , but it happens that $D_3 = A_3$ (a coincidence).

Case (c): The hexagon, which also gives A_3 .

Case (d): What about (d)? Consider the annulus with 3 boundary marked points. A triangulation with arcs τ_1, τ_2, τ_3 and boundary segments $\Delta_1, \Delta_2, \Delta_3$ is shown in Figure 60. Ignoring frozens (i.e. boundary segments), there are 3 triangles. The corresponding quiver is a 3-cycle.

It follows that this quiver has finite mutation type, but infinitely many cluster variables (due to arcs which spiral around the annulus; see Figure 61).



Figure 59: Case (b): the once-punctured triangle, with a triangulation and its corresponding quiver. This gives $D_3 = A_3$.

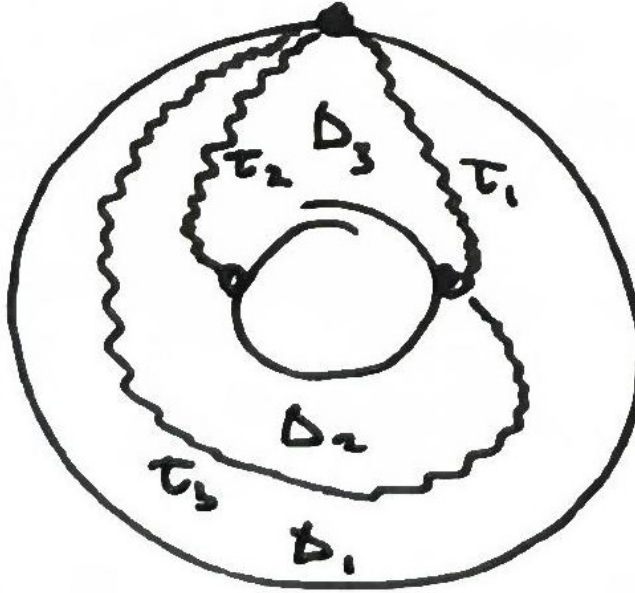


Figure 60: Case (d): the annulus with 3 boundary marked points. The triangulation has arcs τ_1, τ_2, τ_3 and boundary segments $\Delta_1, \Delta_2, \Delta_3$. The three triangles and the corresponding quiver (a 3-cycle) are shown.

13.3 Non-surface-type quivers and infinite mutation type

Example 13.7. Consider the 3-point quiver Q with edge multiplicities 2, 1, 1:



We can show that this is not surface-type, since we already have an exhaustive list of rank 3 surface-type cluster algebras. Alternatively, we will show that the quiver itself has infinite mutation type (which is ruled out in the surface case).

Here is part of the mutation graph (see Figure 62). Continuing in this way with the mutation sequence $\mu_1, \mu_3, \mu_1, \mu_3, \dots$, we see that:

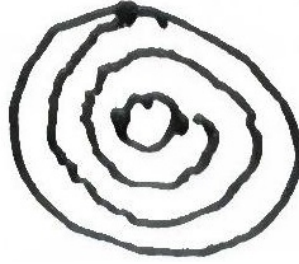


Figure 61: Arcs spiraling around the annulus give rise to infinitely many cluster variables.

- all subsequent quivers are 3-cycles (with each mutation flipping the orientation),
- the total number of arrows increases with each subsequent mutation.

We will think of the total number of arrows as a measure of the “complexity” of the quiver.

More generally, consider the 3-cycle quiver with edge multiplicities x, y, z (see Figure 63), and assume $z > x, y \geq 2$. Then μ_2 gives a new 3-cycle with edge multiplicities $xz - y, x, z$. (μ_3 will be very similar.) Note that

$$xz - y \geq z \quad (\text{i.e. } z(x - 1) \geq y),$$

and the total number of arrows is

$$(xz - y) + x + z > x + y + z,$$

since $xz \geq 2z \geq 2y$.

Lemma 13.8. *Let Q be the 3-cycle quiver with edge multiplicities x, y, z satisfying $z > x, y \geq 2$. Let Γ be the mutation graph of Q , and let Γ' be the connected component of $\Gamma \setminus \{e_Q\}$ containing Q , where e_Q is the edge connecting Q with $\mu_1(Q)$. Then Γ' is an infinite complete 2-ary tree rooted at Q .*

The picture is shown in Figure 64.

Note 13.9. For now, we are taking the vertices of our quivers to be labeled, i.e. we do not identify $1 \rightarrow 2$ with $1 \leftarrow 2$ and so on.

Proof sketch. We have seen that all quivers in Γ' are 3-cycles and the number of arrows increases as we go down in the tree. In particular, for each quiver in Γ' there are exactly two mutations which increase the complexity and one which decreases it.

If Γ' had a cycle, then at the lower “merge point” we would have a quiver such that only one mutation increases the complexity—a contradiction (see Figure 65). \square

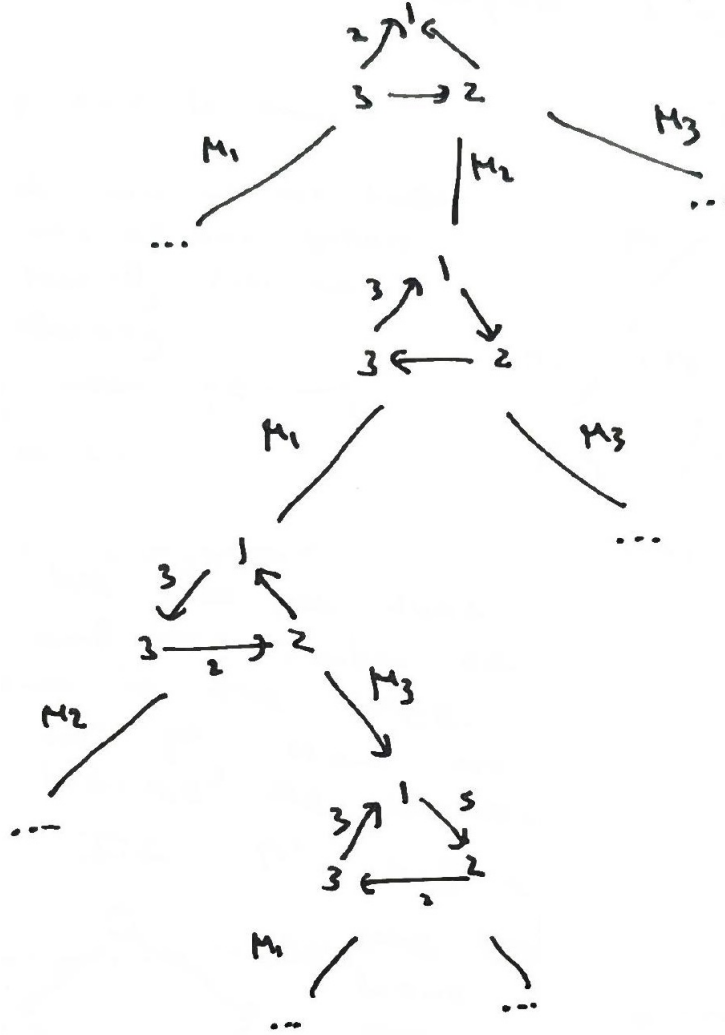


Figure 62: Part of the mutation graph of the 3-cycle quiver with edge multiplicities 2, 1, 1. The total number of arrows increases with each mutation along any branch.

14 Lecture 14

Date: February 27, 2026

Main reference: [War14].

14.1 Forks and the tree lemma

Definition 14.1. A quiver Q is **abundant** if $|b_{ij}| \geq 2$ for all $i \neq j$, where (b_{ij}) is the corresponding skew-symmetric matrix.

Recall that $b_{ij} = \#\{\text{arrows } i \rightarrow j\} - \#\{\text{arrows } j \rightarrow i\}$.

For a vertex k of Q , define full subquivers $Q^\pm(k) \subset Q$, where

- $Q^+(k) = \text{direct successors of } k$ (i.e. those j such that there is an arrow $k \rightarrow j$),
- $Q^-(k) = \text{direct predecessors of } k$.

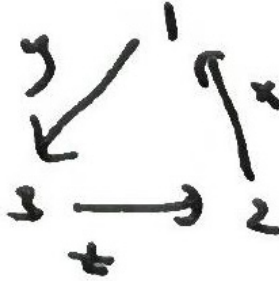


Figure 63: A 3-cycle quiver with edge multiplicities x, y, z (with $z > x, y \geq 2$) and its mutation μ_2 , which produces a 3-cycle with edge multiplicities $xz - y, x, z$.

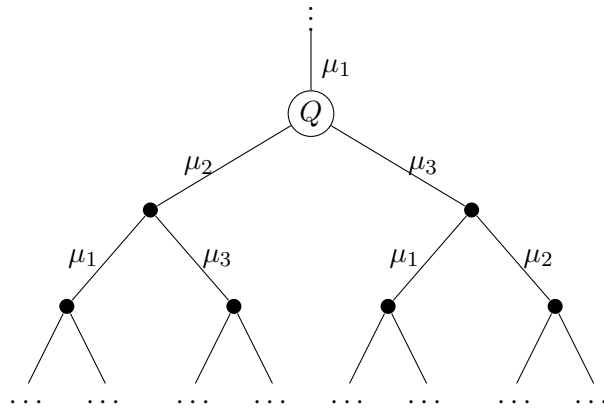


Figure 64: The mutation graph component Γ' is an infinite complete 2-ary tree rooted at Q , with branches corresponding to the mutations $\mu_1, \mu_3, \mu_1, \mu_3, \dots$

Definition 14.2. A quiver Q is a **fork** if it is not acyclic, and there is a vertex r such that:

- (1) Q is abundant,
- (2) for all $i \in Q^-(r), j \in Q^+(r)$, we have $b_{ji} > b_{ir}, b_{rj}$,
- (3) $Q^-(r)$ and $Q^+(r)$ are acyclic.

Here r is called the **point of return**.

Example 14.3. A 3-vertex fork is a cycle with $b_{ji} > b_{ir}, b_{rj} \geq 2$ (see Figure 66).

Note 14.4. Every cycle in a fork must pass through the point of return. Also, the point of return is unique.

Generalizing the lemma from last lecture, we can show that a fork Q gives rise to a tree in its mutation graph.

Lemma 14.5 (Tree lemma). *Let Q be a fork with n vertices and point of return r , and let Γ be the mutation graph of Q . Let e be the edge in Γ joining Q and $\mu_r(Q)$, and let Γ' be the connected component of $\Gamma \setminus \{e\}$ containing Q . Then Γ' is an infinite complete $(n - 1)$ -ary tree rooted at Q .*

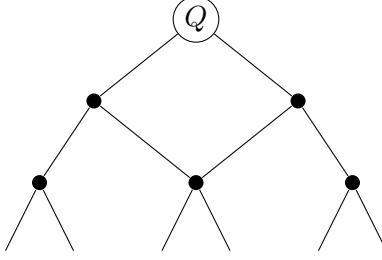


Figure 65: If the mutation graph had a cycle, the quiver at the merge point would have only one complexity-increasing mutation, contradicting the tree structure.

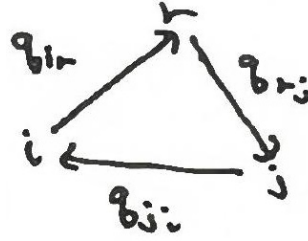


Figure 66: A 3-vertex fork: a cycle with edge multiplicities b_{ir} , b_{rj} , b_{ji} , where r is the point of return.

14.2 Exchange graphs of forks

Note 14.6. Here we are considering mutation and exchange graphs up to permutations of the vertex labels of Q . The exchange graph of an n -vertex quiver is automatically n -regular, but not necessarily the mutation graph.

The tree lemma follows from:

Lemma 14.7. *Let Q be a fork with point of return r , and let $k \neq r$ be another vertex. Then $\mu_k(Q)$ is a fork with point of return r , and $\mu_k(Q)$ has strictly more arrows than Q .*

Corollary 14.8. *Let Q be a fork with n vertices and point of return r . Assume that for all $i \in Q^-(r)$, $j \in Q^+(r)$:*

$$b_{ir}b_{rj} - b_{ji} > b_{ir}, b_{rj}.$$

Then the exchange graph of Q is an n -regular tree.

Proof. The assumption implies that $\mu_r(Q)$ is again a fork with point of return r . Apply the tree lemma twice (see Figure 68). \square

Example 14.9. Consider a 3-vertex fork (a 3-cycle with edge multiplicities b_{ir} , b_{rj} , b_{ji}). The mutation μ_r produces a new 3-cycle with edge multiplicities b_{ir} , b_{rj} , $b_{ir}b_{rj} - b_{ji}$ (see Figure 69). This is a fork if $b_{ir}b_{rj} - b_{ji} > b_{ir}, b_{rj}$.

Definition 14.10. A subgraph of a graph is **convex** if every reduced path with endpoints in the subgraph is entirely contained in the subgraph.

Corollary 14.11. *The forkless part of the exchange graph Γ of any quiver Q is a convex subgraph. In particular, Γ is a tree if and only if the forkless part is.*

Proof idea. Once a path hits a fork, it can never escape it (without backtracking). \square

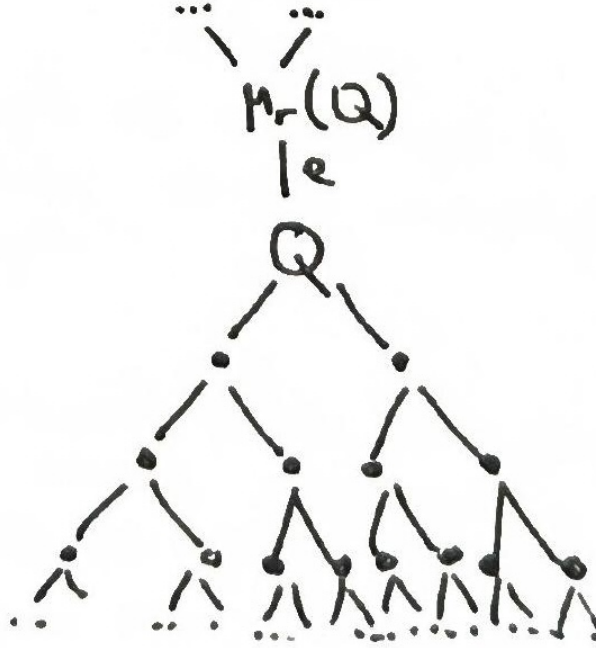


Figure 67: Illustration of the tree lemma: the component Γ' of $\Gamma \setminus \{e\}$ containing Q is an infinite complete $(n - 1)$ -ary tree rooted at Q .

14.3 Mutation-infinite quivers and forks

With similar techniques and some case analysis, one can prove:

Proposition 14.12. *Let Q be a connected quiver with $n \geq 3$ vertices, and i, j vertices such that $|b_{ij}| \geq 3$. Then Q is mutation-equivalent to a fork.*

Remark 14.13. If a quiver Q is mutation-infinite, then after some mutations we can find vertices i, j with $|b_{ij}| \geq 3$, and hence a fork. Thus forks are the only mechanism for mutation-in infiniteness.

Incidentally, to check if a quiver is mutation-infinite, it suffices to check all subquivers with ≤ 10 vertices.

Theorem 14.14 (Felikson–Shapiro–Tumarkin '12). *Any mutation-infinite quiver with ≥ 11 vertices must have a mutation-infinite full proper subquiver.*

14.4 Exchange graphs of mutation-cyclic 3-vertex quivers

We can now state “half” of the computation of exchange graphs of 3-vertex quivers. We say a quiver Q is **mutation-acyclic** if it becomes acyclic after some mutations, and **mutation-cyclic** otherwise.

Theorem 14.15. *Let Q be a 3-vertex quiver which is mutation-cyclic. Then its exchange graph Γ is a 3-regular tree.*

Proof idea. Note that every quiver which is mutation-equivalent to Q is a 3-cycle. WLOG, we can assume $x + y + z$ is minimal (among all quivers mutation-equivalent to Q). Consider the case that Q is a fork, i.e. $z > x, y \geq 2$.

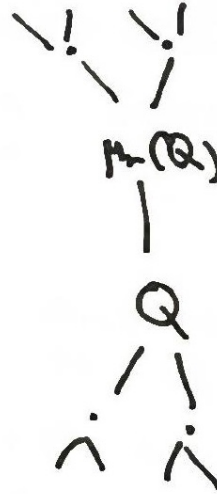


Figure 68: Applying the tree lemma twice: the portion above Q (from $\mu_r(Q)$) and the portion below Q combine to give an n -regular tree.

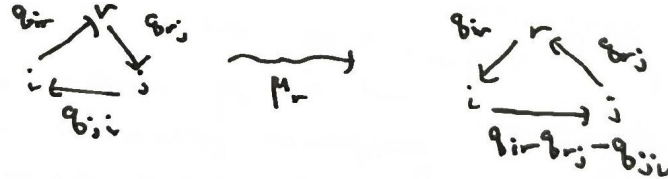


Figure 69: Mutation μ_r of a 3-vertex fork produces a new 3-cycle with edge multiplicities b_{ir} , b_{rj} , $b_{ir}b_{rj} - b_{ji}$.

Then after μ_1 we have a new 3-cycle (see Figure 70). By the minimality assumption,

$$x + y + (xy - z) \geq x + y + z,$$

i.e. $xy - z \geq z > x, y$. It follows by the earlier corollary (Corollary 14.8) that the exchange graph Γ is a 3-regular tree.

Some more work is required for the case $z = y \geq x$. □

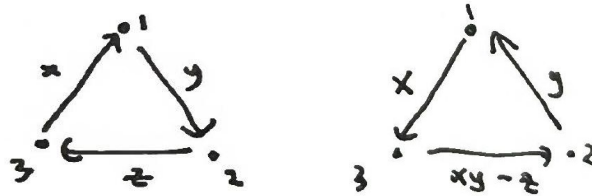


Figure 70: A 3-cycle with edge multiplicities x, y, z (with $z > x, y \geq 2$) and the result of mutation.

Note 14.16. The Markov quiver (a 3-cycle with all edge multiplicities 2) is not a fork, but nevertheless its exchange graph is a 3-regular tree (the Markov tree).

14.5 Alternating mutations

Proposition 14.17. *Let i, j be vertices of a quiver Q . Let Γ be the exchange graph and Γ' the subgraph given by alternating mutations in i and j :*

$$Q - \mu_i(Q) - \mu_j \mu_i(Q) - \mu_i \mu_j \mu_i(Q) - \cdots$$

Then Γ' is:

- a 4-cycle if $|b_{ij}| = 0$,
- a 5-cycle if $|b_{ij}| = 1$,
- or else not a cycle.

Proof idea. The 4-cycle comes from the fact that μ_i and μ_j commute if $|b_{ij}| = 0$. If $|b_{ij}| = 1$, we have the “pentagon relation,” which follows by freezing all other vertices and using the fact that the exchange graph of the A_2 quiver is a 5-cycle. The case $|b_{ij}| \geq 2$ is similar, using the fact that the exchange graph of the m -Kronecker quiver for $m \geq 2$ is infinite. \square

References

- [FWZ21] Sergey Fomin, Lauren Williams, and Andrei Zelevinsky. *Introduction to Cluster Algebras*. Chapters 1–6, arXiv:1608.05735. 2021.
- [Gro+18] Mark Gross, Paul Hacking, Sean Keel, and Maxim Kontsevich. “Canonical bases for cluster algebras”. In: *J. Amer. Math. Soc.* 31.2 (2018), pp. 497–608.
- [War14] Matthias Warkentin. “Exchange Graphs via Quiver Mutation”. PhD thesis. TU Chemnitz, 2014.
- [Wil14] Lauren K. Williams. “Cluster algebras: an introduction”. In: *Bulletin of the American Mathematical Society* 51.1 (2014), pp. 1–26.